STUDIES ON STRUCTURE AND PROPERTIES OF STEEL – ALUMINIUM ALLOY WELD JOINTS BY SPOT WELDING

A DISSERTATION

Submitted in partial fulfilment of the

requirements for the award of the degree

of

MASTER OF TECHNOLOGY

In

Mechanical Engineering

(With Specialization in Welding Engineering)

By

GAUTAM KUMAR SINGH

16542004

MECHANICAL AND INDUSTRIAL ENGINEERING DEPARTMENT

INDIAN INSTITUTE OF TECHNOLOGY ROORKEE,

ROORKEE-247667 (INDIA)

JUNE 2019

Candidate Declaration

I hereby certify that the work which is being presented in this dissertation, entitled, **"Studies on Structure and Properties of Steel- Aluminium Alloy Weld Joints by Spot Welding"** in partial fulfilment of the requirement for the award of the degree of Masters of Technology in Mechanical Engineering with specialization in "**Welding Engineering**", submitted in Mechanical and Industrial Engineering Department, Indian Institute of Technology Roorkee is an authentic record of my own work carried out during the period from June 2017 to June 2019 under the supervision of **Dr. Dheerendra Kumar Dwivedi,** Professor, Mechanical and Industrial Engineering Department, Indian Institute of Technology, Roorkee, India.

I have not submitted the matter embodied in this report for award of any other degree.

Dated: 24-06-2019 **Gautam Kumar Singh**

Place: Roorkee **Enrolment No. 16542004**

Certificate

This is to certify that the above statement made by the candidate is correct to the best of my knowledge.

Dr. Dheerendra Kumar Dwivedi
Professor, MIED
IIT Roorkee

Acknowledgement

I wish to express my deep sense of gratitude and sincere thanks to **Dr. Dheerendra Kumar Dwivedi,** Professor in the department of MIED, IIT Roorkee for being helpful and a great source of inspiration. I would like to thank him for providing me with an opportunity to work on this excellent and innovative field of research. His keen interest and constant encouragement gave me the confidence to complete my work. I wish to thank him for their constant guidance and suggestions without which I could not have successfully completed this dissertation work

I am very thankful to Mr. Anup Kulkarni and Mr. Pankaj Kaushik (research scholars- MIED, IIT Roorkee) for their never-ending assistance during completion of experimental work and bringing out this dissertation report.

Also, I would like to thank my parents, all teaching and non-teaching staffs of the department, and my friends who have contributed directly or indirectly in successful completion of my dissertation work.

Gautam Kumar Singh

Enrolment No. – 16542004

M. Tech – 2nd Year (Part Time)

(Welding Engineering)

Abstract

Al 5052- H32 (1.5 mm thick) alloy welded with Zn coated galvannealed steel (1.0 mm thick) by resistance spot welding with and without use of cover plate (CRC steel- 1.0 mm thick) with the objective of to achieve higher strength of joint at lower range of welding current. Effect of Zn coating on microstructure and mechanical behaviour of joint was explored and effect of nugget diameter, and thickness of reaction layer on tensile shear strength was discussed.

Macrostructure of joint cross section and fractured surface were inspected using stereo microscopy, while microstructure and intermetallic layers were analysed using optical and field emission scanning electron microscopy. Shear tensile test was carried out at universal testing machine of 100 KN capacity and nugget diameter was measured from fractured surface.

Fluxing action of Zn ensures thinner uniform reaction layers and good metallurgical bonding at low temperature. Reaction layer thickness is maximum at nugget centre and decrease with distance from centre for both joint. With increase of welding current, thickness of reaction layer slightly increases for joint without cover plate and drastically reduces for joint with cover plate. Nugget diameter and shear tensile strength increased for both joint with increasing current. However, joint with cover plate have higher growth rate of nugget diameter due to availability of some additional heat at interface conducted from cover plate. Excess increase in nugget diameter and reduction in thickness of intermetallic layer is the reason for dramatic improvement in shear strength for joint with cover plate. Maximum tensile shear load is 5675 N at 10.0 kA for joint with cover plate and 4049.3 N at 11.0 kA for joint without cover plate i.e. 40.14 % improvement in joint shear strength with the use of cover plate.

Table of Contents

List of Figure

List of Tables

Abbreviations

Abbreviation	Description
RSW	Resistance spot welding
HAZ	Heat affected zone
BM	Base metal
FZ	Fusion zone
UTS	Ultimate tensile strength
SEM	Scanning electron microscope

Chapter 1

Introduction

1.1 General Background

Increased demand for energy of growing population and global warming caused mainly by emission of greenhouse gases such CO_2 emission from burning of fuels, are the global problem.

There is direct relation between energy, environment, and sustainable development. A country seeking sustainable development ideally must utilize only those energy resources which have minimal environmental effect. Some of the limitations imposed on sustainable development by environmental emission and their negative impact in a part be overcome through conserving energy.

Industrial sector (viz. automobile, marine, aircraft, cooling amenities, etc.) continues to be the highest energy consuming domain where energy conservation would play a vital role to address the problem.

Automotive industries have taken enormous effort to improve fuel consumption by reducing car weight. This reduction in car weight can be attain by the combined use of high strength steel and light weight material such as Al, Mg, carbon fibre reinforcement polymer, etc. in the structure of car body. However, it is difficult to use low density material for the entire vehicle body structure from the view point of cost and productivity, therefore multi-materials light weight structure design tactics is used in which both lighter materials and high strength are being used to achieve improve fuel consumption.

However, joining of light weight material Al with steel by conventional fusion welding faces metallurgical and technological problem during welding. Difference between their physical properties such as thermal conductivity, coefficient of thermal expansion, and melting point cause weld defect such as solidification cracking, porosity at interface. Limited mutual solubility of Al and steel result in formation brittle intermetallic compounds (IMCs) at interface are some obstacles for good quality of weld.

One of prime issue during welding of steel with aluminium is removal of oxide layer from the surface of Al and steel. Zn coating between Al and steel play a vital role in removal oxide layer by fluxing behaviour of Zn. Zn reacts with Al and formed binary eutectic alloy, who's melting point is lower than that of base metals. Eutectic liquid containing oxide is discharged at nugget

periphery by electrode force, and thus leaving a clean steel surface for lower temperature metallurgical bonding.

Because of simplicity, high efficiency (low process time), adaptability, and automation possibility for high productivity, resistance spot welding (RSW) is the most commonly used welding method in automotive industry for the manufacturing of vehicle body and component.

1.2 Resistance Spot Welding

Spot welding is a resistance welding process in which coalescence of metal is produced at the faying surfaces by the resistance heating of base metal due to the flow of electric current. Force is continuously applied before, during, and after the application of current to prevent arcing at the faying surfaces and in some applications to forge the weld metal during post heating to reduce porosity and hot cracking in the weld nugget. The process is completed within a prescribed weld cycle (squeeze time, weld time, and hold time). Melting occurs at the faying surface during weld time. A nugget of weld metal is produced at the electrode site.

Sequence of operation should first develop heat to raise the confined volume of metal to the molten state then cools the molten metal under applied electrode force until joint has adequate strength.

Current density, and pressure should be such that a nugget is formed. It should not be so high that molten metal will be expelled from the weld zone. Weld time must be sufficiently short to prevent excessive heating of electrode faces. Such heating can bond the electrode with the parts and thus can cause rapid electrode deterioration.

Fig. 1 illustrates the process. Fig. 2 represent basic electrode cycle.

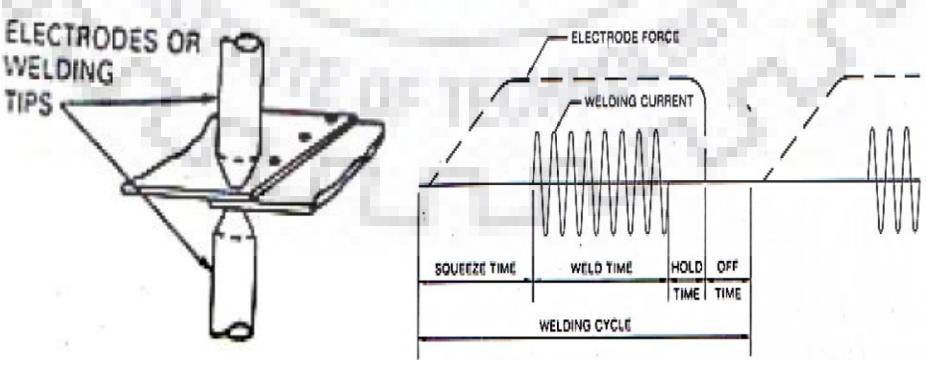

Fig. 1 Resistance spot welding (Keran, 1980) [1]. **Fig. 2** Basic weld cycle for spot welding (Keran, 1980) [1].

In the present study Zn based coating steel (galvannealed steel) have been welded with Al 5052 alloy with and without cover plate (CRC steel) using resistance spot welding. Effect of welding

current and Zn coating on the interfacial microstructure and joint properties has critically examined and obtained results have been analysed and compared for both joint with and without cover plate.

Chapter 2

Literature Survey

2.1 Metallurgical Challenges During RSW of Al/Steel

Following metallurgical phenomena occurs during the RSW of Al/steel-

1.) Melting Phenomena in the BMs and solid/liquid or liquid/liquid interface

Due to high thermal conductivity of Al, coupled with high thermal gradient between Al and steel, part of the resistance heat generated in the steel is conducted into Al sheet. This excess heat along with lower melting point of Al leads to the melting of Al and liquid nugget formation in the Al sheet. [9]

Liquid/solid interface is obtained which suggest that metallurgical bonding is achieved by brazing mechanism. Depending upon the high heat generated in the steel sheet, a separate liquid nugget may be formed in the steel sheet and liquid/liquid interface is obtained at the interface.

2.) Wetting of solid steel by liquid aluminum

Contact resistance at the interface is affected by oxide, foreign material, dirt, and oil on the surface. Presence of oxide and foreign material can affect the wettability of surface. To get the uniform weld properties, surface must be cleaned.

In RSW, combined effect of electrode force and resistance heat at the interface, broke up the oxide layer. Wetting is usually confirmed where surfaces are clean. Oxide film also removed by applying some coating such as Zn on steel. During the heating, Zn is rapidly dissolved by Al and formed binary eutectic liquid alloy of Al-Zn through lower temperature eutectic reaction, providing a clean steel surface, ensure good wetting, and thus uniform weld properties. [11]

3.) Formation of intermetallic compound: prime issue in Al/steel joining

Binary Fe/Al equilibrium phase diagram is represented in Fig. 3. Al has limited mutual solubility in Fe and range of intermetallic phases are possible via dissolution of base metals, e.g. $FeAl_3$, Fe_2Al_5, $FeAl_2$, Fe_3Al and FeAl.

Fig. 4 illustrates the macrostructure of RSW of steel/Al along with interfacial reaction.

Aluminium rich intermetallic compounds (Fe_2Al_5) have lower symmetrical crystal structure [9], hence Al rich IMCs are more brittle than Fe- rich IMCs (Fe_3Al). Diffusivity of Al in Fe is much higher than Fe in Al, so formation of Al rich intermetallic ($FeAl_3$, Fe_2Al_5) are promoted at the faying surfaces of Al/steel as shown in Fig. 4. Internal stresses created during joining dur large difference of thermal properties of base metals. Brittle IMCs coupled with these internal stresses are susceptible for brittle failure during service.

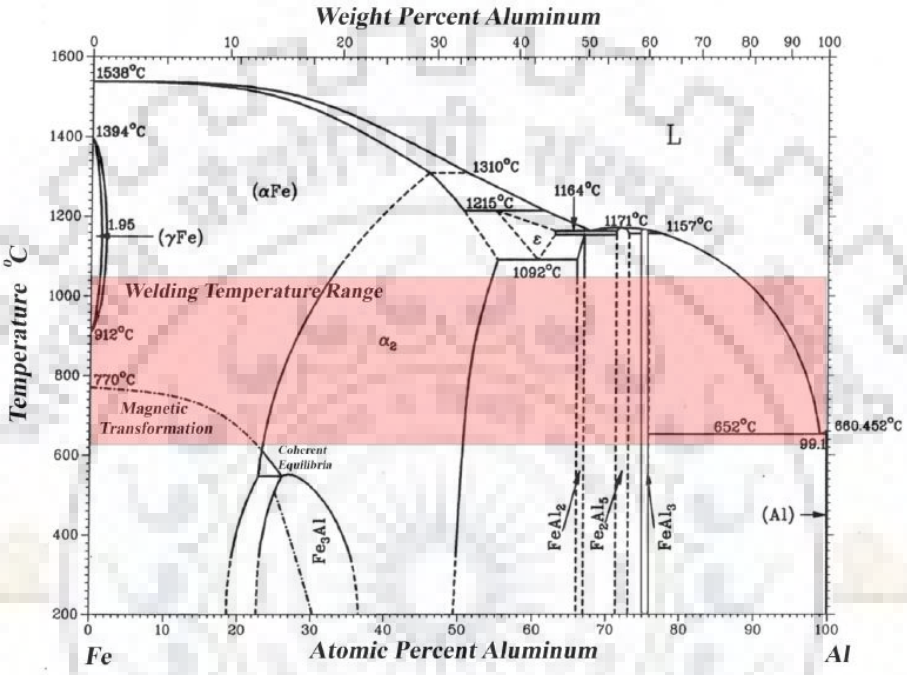

Fig. 3 Binary Al- Fe phase diagram (Mazar et al., 2014) [8].

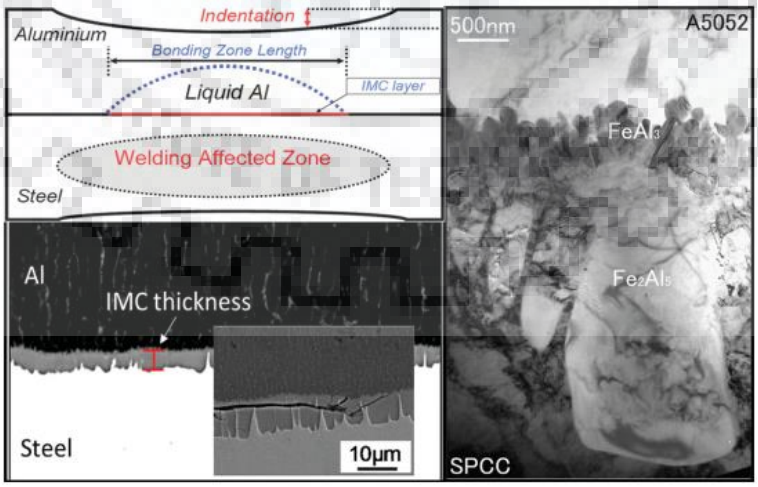

Fig. 4 Macrostructure of dissimilar RSW of Al/steel along with interfacial reaction (Pouranvari, 2017) [9].

2.2 Factors governing the tensile shear strength of Al/Steel RSW

Factors controlling the mechanical property of joint is summarised as follows-

1.) Bonding zone length (diameter of nugget)

It is the diameter of liquid Al nugget at the interface, which is function of welding heat input. This determine the load bearing area as shown in Fig. 4.

2.) Thickness of IMC layer

Controlling the growth of brittle IMC is key to develop reliable joint. The thickness of IMC primarily depends upon-

i.) Welding heat input i.e. peak temperature at the interface

ii.) Composition of base metals (steel, Al)

iii.) Composition of coating on steel

3.) Electrode indentation in Al sheet

Electrode face geometry determines the pressure and current density. Excessive heating (due to high current density and/or weld time) cause overheat of base metals and result in deep indentation, which affects the state of stress and thus influences the mechanical strength of the joint. This factor is governed by heat input, electrode geometry, and electrode force.

4.) Defects created at the interface of steel/Al

Porosity/void is formed in Al nugget, which is caused by-

i) Solidification shrinkage and weld metal expulsion

ii) Steel vaporization and improper wetting, where reaction layers is discontinued due to uneven removal of oxide layer.

2.3 Experimental Investigation

2.3.1 Effect of welding current and time on bonding zone length (nugget size) [6]

Amount of volume melted at the faying surfaces is function of heat input.

In the formula, $Q = I^2Rt$, current has major effect on the generation of heat than resistance or time. So current is a crucial variable to be controlled.

Heat is increases by increasing the welding current and/or time, which increases nugget diameter.

As expressed in Fig. 5 and 6, slope of nugget growth is not constant for all values of current. As the welding current and time increases, weld nugget diameter increases almost linearly. But after some value of current and time, it indicates a gradual change, because of equilibrium between resistance heat input and heat loss.

Two parameter governs the growth of nugget diameter –

i.) Rise in electrical resistance due to increase of temperature in weld nugget

ii.) Reduction in electrical resistance due to enlargement of nugget diameter

At beginning, welding heat (due to increase in welding time/current) has more prominent effect because of smaller size of nugget. As the nugget size increases, it reduces the electrical resistance which limits the growth rate of nugget. Therefore, nugget size remains almost constant for high welding current/time.

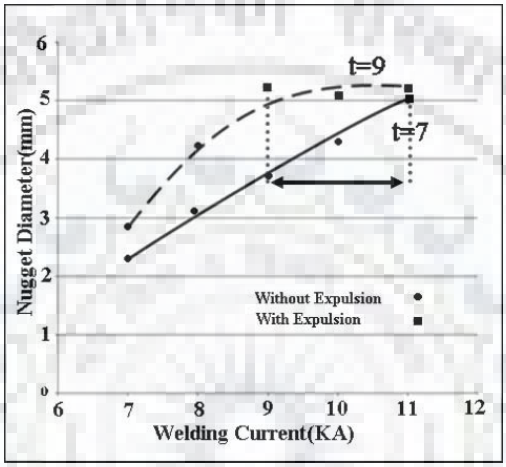

Fig. 5 Nugget size variations w.r.t. current (Pouranvari et al., 2007) [6].

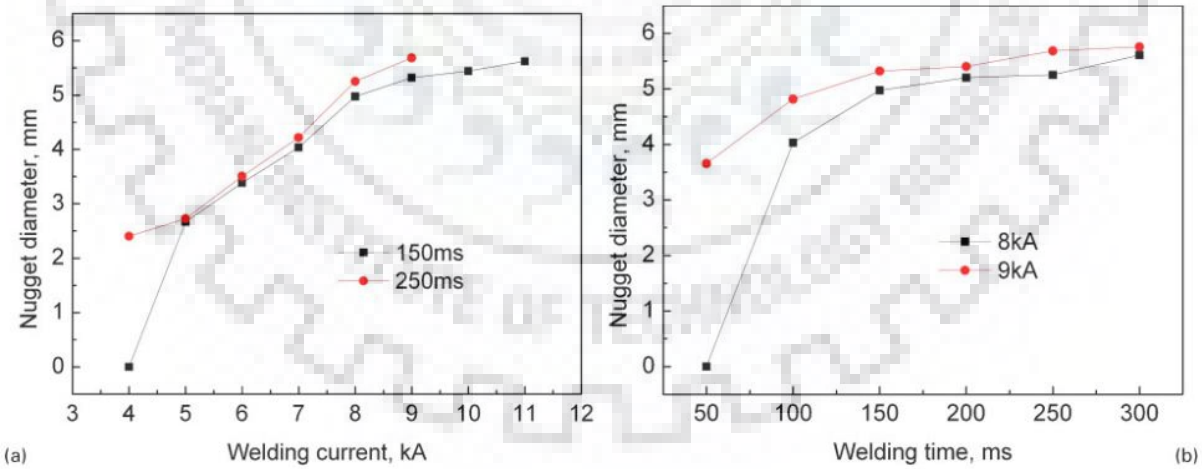

Fig. 6 Effect of welding parameter on nugget size (Zhang et al., 2011) [10].

2.3.2 Effect of holding time on nugget diameter

Table 1 expressed that nugget diameter is almost constant for all the holding time. Since electrode holding does not affect the heat input at faying surfaces, therefore hold time does not change the amount of molten volume. [6]

Table 1

Effect of holding time on nugget size, failure mode, and peak load

(Pouranvari et al., 2007) [6].

Holding time, cycles	Nugget diameter, mm	Peak load, kN	Failure mode
0	3·60	4·32	PF
5	3·65	4·30	PF
20	3·70	4·40	PF
50	3·60	4·25	PF
90	3·65	4·40	PF

*PF is the pullout failure mode.

2.3.3 Effect of electrode pressure on nugget size

Table 2 shows that nugget size decreases with the increase of electrode force. Increase in electrode force, reduces sheets thickness between electrodes, enlarged the contact area at the joint interface.

$$R = \rho * L/A$$

Increase in electrode pressure will reduce contact resistance at the joint interface due to enlargement of contact area. Reduction in contact area reduces the resistance heat input at the interface and thus, reduction of nugget size.

Table 2

Effect of electrode pressure on nugget size, failure mode, and peak load

(Pouranvari et al., 2007) [6].

Electrode pressure, bar	Nugget diameter, mm	Peak load, kN	Failure mode
2·5	4·20	4·56	PF
3·0	3·65	4·30	PF
3·3	2·67	4·00	IF
3·5	2·50	3·66	IF
4·5	2·10	2·56	IF

*PF is pullout failure mode and IF is interfacial failure mode.

2.4 Microstructural analysis

2.4.1 Joint appearance

Figure 7 revealed the cross-sections of the welded joints under different welding conditions. As it can be seen, reaction took place between molten aluminium and solid surface of galvanised steel. Hence the welded joint is composed of a melted aluminium alloy nugget and a steel heat affected zone, and it could be regarded as solid liquid interface (brazing mechanism).

With increasing the welding current and time, welding heat will increase, which result in expansion of molten Al alloy, and also indentation depth increased simultaneously. Molten Al alloy introduced into galvanised steel at the centre of weld joint (bulging of Al).

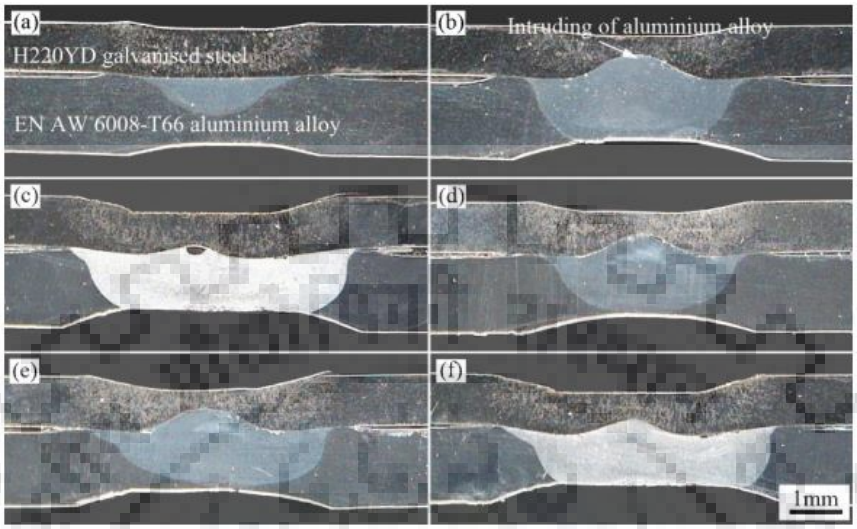

a 5 kA, 250 ms; *b* 7 kA, 250 ms; *c* 9 kA, 250 ms; *d* 8 kA, 100 ms; *e* 8 kA, 200 ms; *f* 8 kA, 300 ms

Fig. 7 Cross-sections of welded joints at different welding currents and welding times (Zhang et al., 2011) [10].

2.4.2 Morphology of reaction products (IMCs) at the welding interface [10]

Fig. 8 is the optical and SEM microstructures of the joint, and analysis positions are plotted from E to G. Reaction layers (IMCs) were formed at the Al/steel interface, and the microstructure and thickness variation of reaction layers at interface is plotted in Fig. 8f–h.

Reaction layer is thicker at the centre and its decreases with the distance from the centre. Finally, it becomes discontinuous at the centre. [10]

At the weld centre, two layered structure of IMC in thickness direction plotted as I and II, as shown in Fig. 8f. Reaction products front showed compact lath structure beside the galvanised steel (layer I), and long needle-like phases oriented towards the aluminium alloy nugget, as certain needles interspersed in the nugget (layer II).

At the intermediate region (between the weld centre and periphery) reaction products exhibit the tongue-like morphology in the galvanised steel side and an extremely fine needle-like reaction product oriented towards aluminium alloy side (Fig. 8g).

Figure 6h showed a thinner interfacial layer at the peripheral region of the weld.

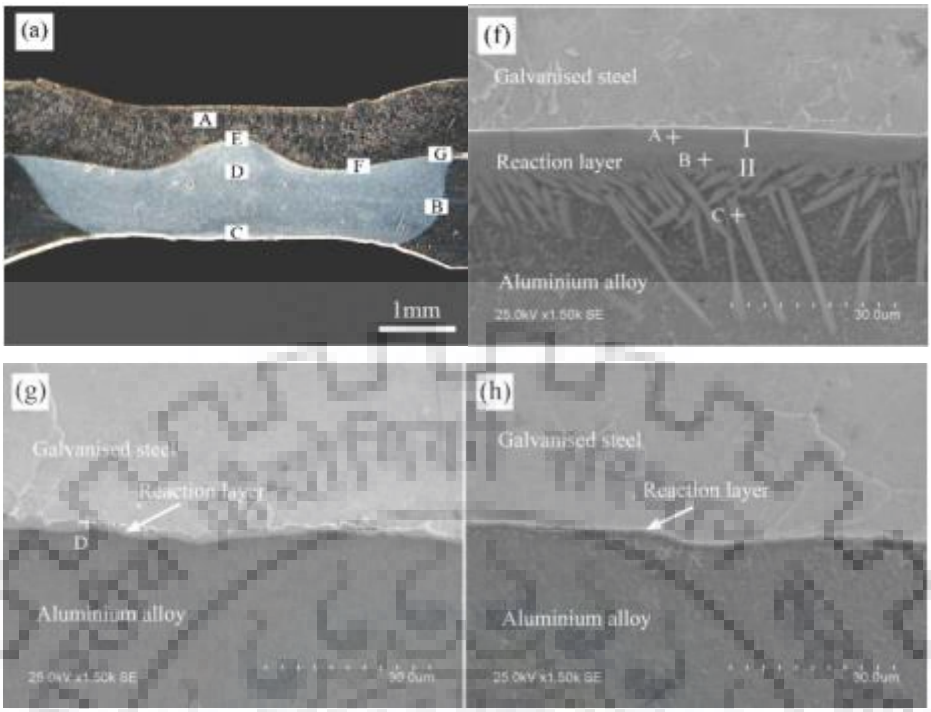

Analysis positions: (f) E zone, (g) F zone, (h) G zone

Fig. 8 Optical and SEM microstructures of welded joint (Zhang et al., 2011) [10].

2.4.3 Microstructure of reaction product

Fig. 9 expressed a two-layered structure, which is consisted of a large mono-crystalline layer adjacent to the SPCC, and a polycrystalline layer adjacent to the A5052. Mono crystalline layer composed of a tongue- like structure oriented towards SPCC and polycrystalline layer is composed of fine needle like structure oriented towards A5052. By EDX analysis It was identified that these layers are Al rich IMCs. The fine crystal grains were $FeAl_3$ and the large one was Fe_2Al_5. [5]

Origin of formation of Al rich intermetallic (tongue like Fe_2Al_5) is still unclear, but anisotropic diffusion is possible explanation for it. There is large number of vacancies of Al along c- axis of orthorhombic structure of Fe_2Al_5. There is fast diffusion of active element along c- axis, result in anisotropic growth of Fe_2Al_5

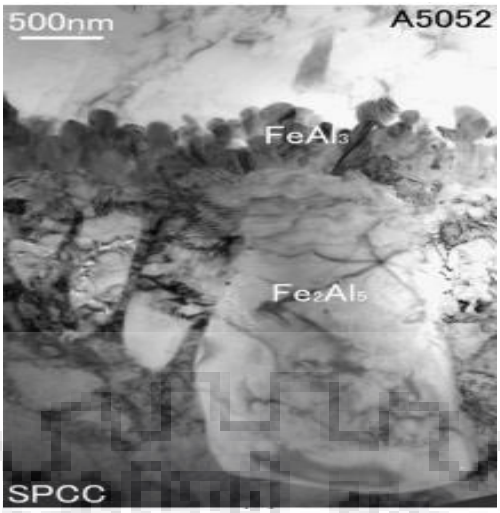

Fig. 9 TEM image of weld cross section at A5052/SPCC welding interface (Qiu et al., 2009) [5].

2.5 Effect of welding current and time on reaction layer thickness

Reaction layer is function of welding heat input i.e. interaction time (t) and temperature at the interface ($T_{S/L}$). Temperature is high at the central region and decrease with the distance from centre due to heat loss. Hence reaction layer is thicker at the centre and decreases with the distance from the centre as shown in Fig. 10. [5,10]

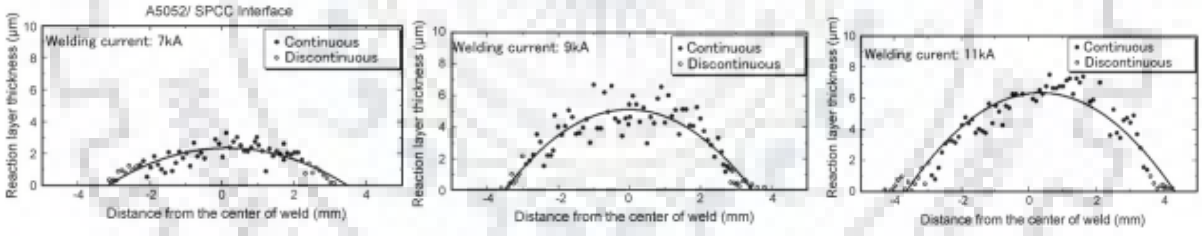

Fig. 10 Distribution chart of reaction products layer thickness at the welding interface of A5052/SPCC (Qiu et al., 2009) [5].

Fig. 10 and 11 showed, reaction layer thickness increased with increasing of welding current because welding temperature increased with the increasing of welding current.

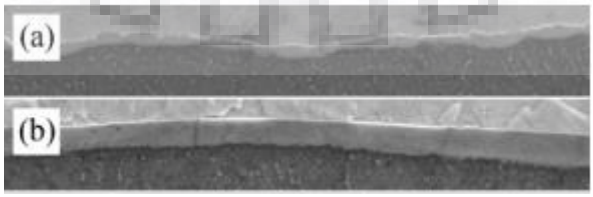

a 100 ms, 9 kA; b 200 ms, 9 kA;

Fig. 11 Microstructures (SEM) of joint at central region of galvanised steel/aluminium alloy interface at different welding currents (Zhang et al., 2011) [10].

Fig. 12 shows reaction layer thickness increased with increasing welding time. Higher temperature/ time (high heat input) facilitate anisotropic diffusion of Al atom into steel, and provide more energy for reaction between Al and Fe atoms. As the welding temperature increased at the interface by means of increasing welding current and/or time, Al atom had sufficient activation energy to overcome reaction layer and react with Fe atoms, resulting more thicker reaction layer of IMCs with more lath/flat feature in the galvanised steel side.

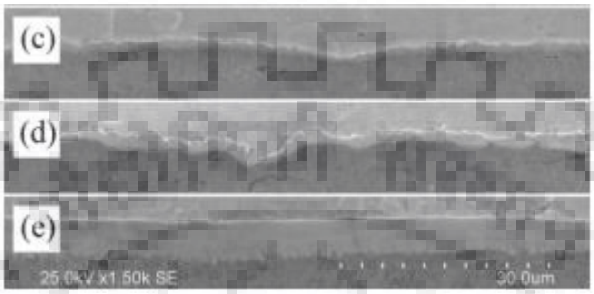

(c) 5 kA, 250 ms; (d) 7 kA, 250 ms; (e) 9 kA, 250 ms

Fig. 12 Microstructures (SEM) of joint at central region of galvanised steel/aluminium alloy interface at different welding time (Zhang et al., 2011) [10].

2.6 Effect of welding current and time on tensile shear load

Although tensile shear strength depends on sheet thickness, level of weld porosity, local microstructural changes, formation of IMCs, and nugget diameter. But nugget diameter is most important criterion to determine the weld strength. [6, 10]

Fig. 5 and 6 express that as the welding current and time increased, weld nugget increases almost linearly i.e. bonding zone length (load bearing area) increased. Hence tensile shear load increased in a quasi linear characteristic as shown in Fig. 13 and 14.

Fig. 13 and 14 also expressed, there is dramatic improvement in shear strength at higher welding current and/or time, and it is almost constant for higher value of current and/or time, since there is no significant improvement in nugget diameter, as growth rate of nugget diameter is very slow and almost constant for higher value of current and/or time as indicated in Fig. 4 and 5.

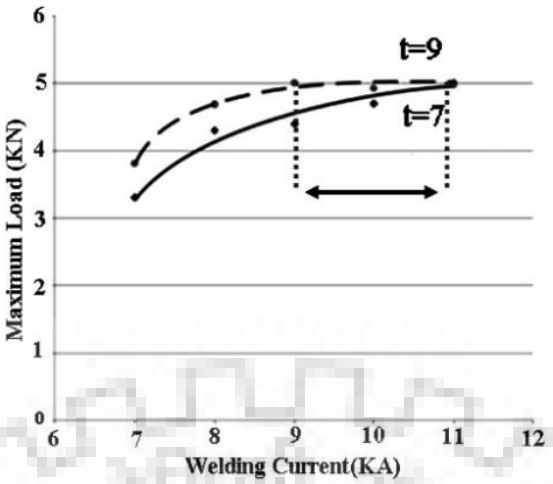

Fig. 13 Maximum load variation versus welding current (Pouranvari et al., 2007) [6].

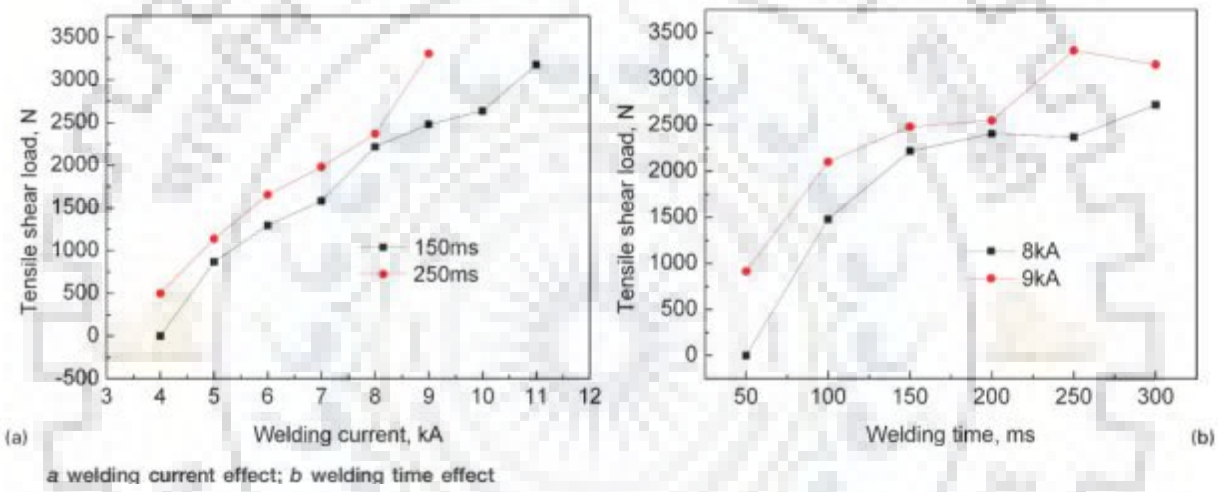

Fig. 14 Effect of welding parameter on joint strength (Zhang et al., 2011) [10].

2.7 Effect of welding current and time on indentation size

Fig. 15 shows increased of welding current and time result in gradual increment in joint thickness percentage reduction. As the heat input increased, molten Al alloy also increased and galvanised steel with high temperature were acquired. Which result in high depth of indentation size, hence percentage thickness reduction also increased with increased of heat input by means of increasing welding current/time. [10]

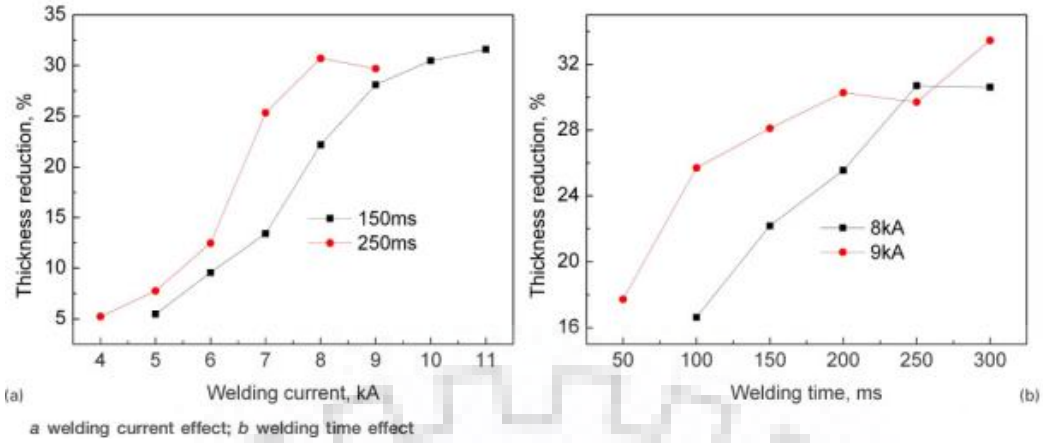

Fig. 15 Effect of welding current and time on joint thickness reduction
(Zhang et al., 2011) [10].

2.8 Failure mode

Generally, there is mainly two kind of spot weld failure- [6, 9]

1.) Interfacial failure mode
2.) Pullout failure mode / Plug type fracture

In interfacial mode, failure propagate through nugget, while in pullout mode, failure occurs through complete/partial removal of nugget from one sheet as noticed in Fig. 16.

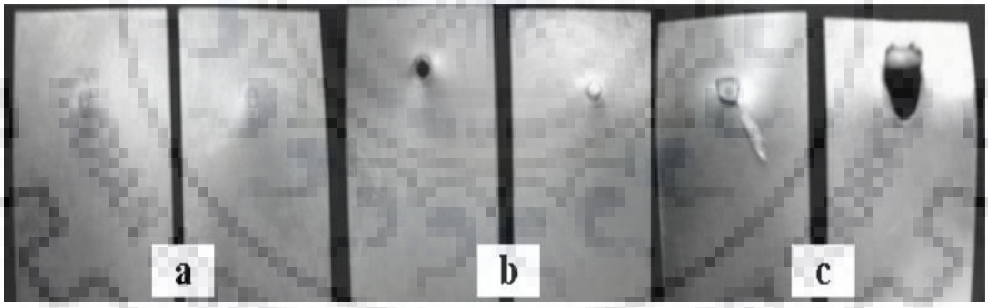

Fig. 16 Different types of failure modes (a) interfacial, (b) pullout, (c) partial pullout followed by base metal tearing
(Pouranvari et al., 2007) [6].

Load extension curve for both failure mode under tensile shaer test is shown in Fig. 17.
Load carrying capacity (energy absorption capability) of spot weld failed under pullout mode is much higher than those failed under interfacial mode.
To ensure the reliability of spot weld, process parameter should be adjusted in such a way that pullout mode can be achieved.

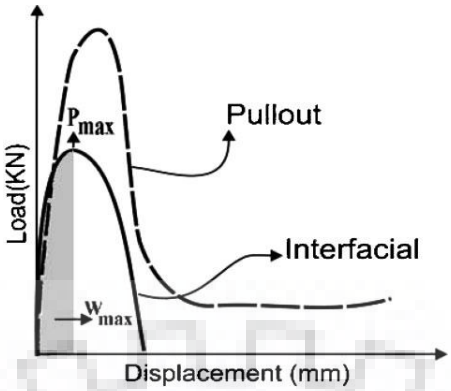

Fig. 17 Load displacement diagram for both failure modes (Pouranvari et al., 2007) [6].

1.) Interfacial failure mode

Interfacial failure occurs in two ways

i.) Failure occurs through nugget i.e. through reaction layer when thickness of IMC is greater than critical value.

Fig. 18 shows SEM images of interfacial region failed under tensile shear. Crack initiated in reaction layer at the interface (Fig. 18 a), and propagated through brittle reaction layer at the weld centre i.e. failure occur through IMC layer.

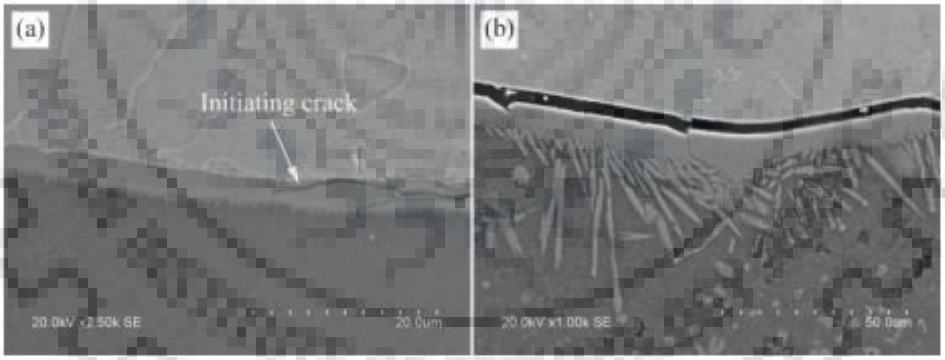

a initiating crack at interfacial intermetallic compound layer; *b* fractured layer

Fig. 18 Interfacial region of partially tensile shear failed of AW 6008- T66/galvanised steel joint (Zhang et al., 2011) [10].

In case of fracture through intermetallic layer, fractured surfaced were very flat as observed the fracture surfaces of fractured A5052/SPCC joint in Fig.19.

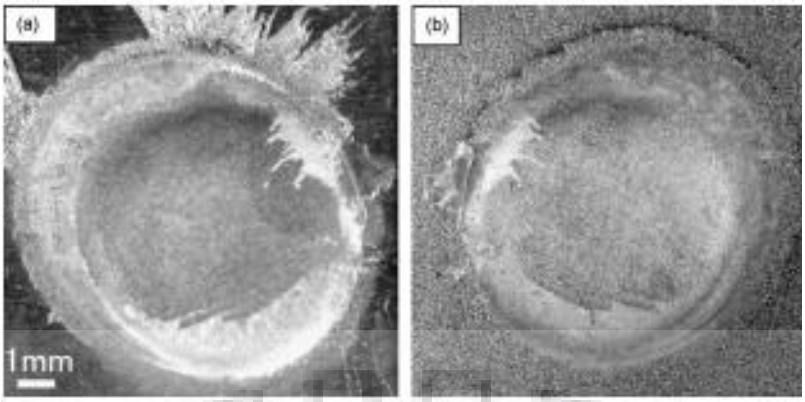

Fig.19 (a) A5052 side (b) SPCC side fracture surfaces of fractured A5052/SPCC joint (Qiu et al., 2009) [5].

ii.) Failure occurs via rupture between Al sheet and intermetallic layer when the IMC is very thin and discontinuities (pores/void, un- bonded region) are present at weld interface.

Fig. 20 (c) indicates fracture crack propagated between Al sheet and intermetallic layer also tear dimple features were observed on both fractured surfaces as shown in Fi. 20 (a) and (b).

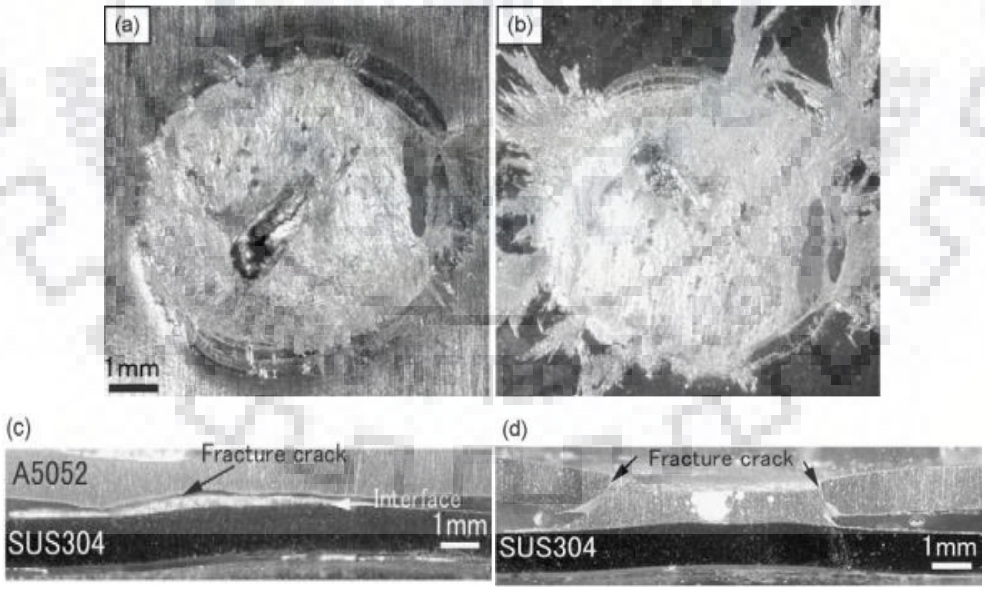

Fig. 20 (a) A5052 side, (b) SUS304 side fracture surface and (c) cross-section of shear fractured of A5052/SUS304 joint (d) cross- section of plug fractured of A5052/SUS304 joint (Qiu et al., 2009) [5].

2.) Pullout failure mode

In pullout failure mode nugget withdrawal (complete or partial) from one of Al sheet when large nugget diameter (bonding zone/load bearing area) couples with thin reaction layer (IMC) as shown in Fig. 20 (d). It is clear that crack propagate through Al sheet and it did not propagate through intermetallic/reaction layer.

2.8.1 Effect of welding parameter on failure mode

As per result shown in Table 3, interfacial failure occurs for low welding time and current, while it changed to pullout mode for higher welding current and time. This is because of increasing nugget diameter with increasing current and time as shown in Fig. 5 and Table 1. Joint A5052/SUS304 [5] shows interfacial failure mode at lower welding current as shown in Fig. 20 (c) and transformed to pollout mode at higher current as displayed in Fig. 20 (d). [6]

Table 3

Effect of welding current and time on nugget size, failure mode, and peak load (Pouranvari et al., 2007) [6].

			Welding conditions†					Welding conditions†	
Failure mode	Peak load, kN	Nugget diameter, mm	Welding time, cycles	Welding current, kA	Failure mode	Peak load, kN	Nugget diameter, mm	Welding time, cycles	Welding current, kA
IF	3·2	2·2	7	7	IF	3·7	2·4	5	8
IF	4·2	3·1	7	8	IF	4	2·8	6	8
PF	4·5	3·8	7	9	IF	4·2	3·1	7	8
PF	4·8	4·2	7	10	PF	4·3	3·65	8	8
PF	5	5	7	11	PF	4·8	4·2	9	8
IF	3·8	2·8	9	7	PF	4.	3·5	5	9
PF	4·8	4·2	9	8	PF	4·2	3·7	6	9
PF	5	5·2	9	9	PF	4·5	3·8	7	9
PF	4·9	5·1	9	10	PF	5	5·1	8	9
PF	5	5·2	9	11	PF	5	5·2	9	9

*IF is interfacial failure mode and PF is pullout failure mode.
†In all cases the holding time is 5 cycles and the electrode pressure is 3 bar.

2.8.2 Weld failure mechanism

Under applied shear load, first nugget rotates in order to orient with applied force direction and stresses are distributed around weld circumferences and at the interface/centre line. Nature of stress is shear at weld interface and tensile around weld circumference. [6]

In pullout failure mode, induced tensile stress at weld circumference is dominant over shear stress at interface, which cause uneven necking in both sheets. If this necking is continuously stressed under applied shear force, the nugget will eventually withdraw/ shear off from one of the sheets. Although the loading mode is shear, but mechanism of failure has tensile nature in pullout mode. Ductile fracture under tensile shear load is confirmed by dimples in facture surface as indicated in Fig. 21 (a).

In interfacial failure mode, shear stress at interface is dominant over induced tensile stresses at weld circumference. As the shear stress exceed the nugget shear strength, before induced

tensile stress cause necking in the sheets, weld is failed at interface. Elongated dimples are shown in Fig. 21 (b), which confirms that the failure mechanism is shear.

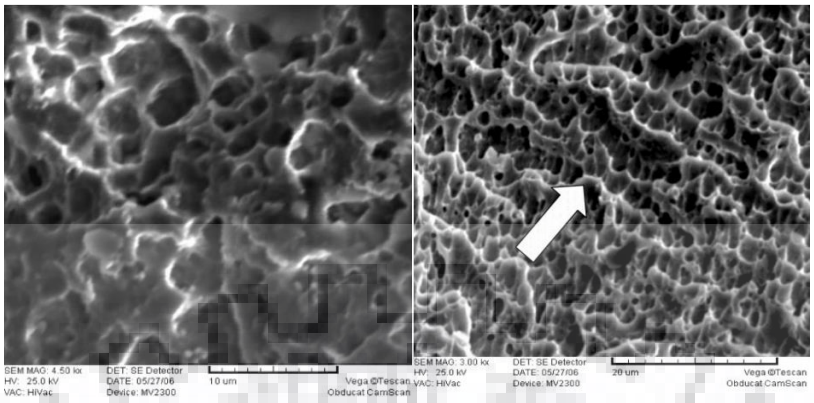

Fig. 21 SEM image of fracture surface of spot weld failed in (a) pullout mode (b) interfacial mode (Pouranvari et al., 2007) [6].

2.9 Recent work: approach to improve joint properties

Recent work done by researchers to improve joint properties are represented as follows-

2.9.1 Cover plate: for controlling L/S interface temp

In 2009, Qiu et al. [5] joined A5052/SPCC and A5052/SUS304 with cover plate (SPCC) technique. Cover plate is placed on Al sheet, which have relatively low electrical and thermal conductivity than aluminium alloy, so the higher heat generated in cover plate is directed towards aluminium/steel interface resulting an increase of interface temperature $T_{L/S}$ (200-300℃ higher temperature obtained when welding without cover plate), and thus enlarged the bonding zone.

This study reported-

i.) Larger nugget diameter (at 9KA,10mm for A5052/SUS304 AND 8.9mm for A5052/SPCC) and high strength (6.5KN for A5052/SUS304 and 4.68KN for A5052/SPCC) were obtained at relatively low current.

ii.) Aluminum rich reaction product (Fe_2Al_5, $FeAl_3$) were observed at the interface and reaction layer thickness varies with the welding current, and position. Maximum thickness appeared at the central region (at 11KA, 7μm for A5052/SPCC AND 2.5μm for A5052/SUS304). This minimum thickness of reaction layer for A5052/SUS304 due to presence of Cr in SUS304, which inhibit the anisotropic growth of Al atom.

Advantage of using this technique is enhanced mechanical property caused by enlarging bonding zone (nugget diameter) at relatively low current. Thus, low electrode indentation and degradation. This technique does not report remarkable impact on growth of reaction layer.

2.9.2 Zinc Coating: Improving Wetting by Fluxing Action

In 2017, Pouranvari [9] analysed that unwetted/un- bonded regions due to presence of Al oxide layer at the interface is key issue to obtain stronger bond in RSW of Al/steel joint. Removal of oxide layer requires high current/time (heat input) under applied electrode force. But it results in formation of thick reaction layer (IMC) at the interface.

Presence of Zn coating is beneficial for RSW of steel/Al joint due to two feature-

i.) **Fluxing behavior:** As shown in Fig. 22, oxide film is destroyed under applied electrode force and heat. Al and Zn reacts and eutectic liquid of Al- Zn is formed through low temperature eutectic reaction at the joint interface, and removed the oxide layer. Eutectic liquid containing oxide is discharged at nugget periphery by electrode force, and thus leaving a clean steel surface and ensuring good wetting, thus more uniform Al rich reaction layer forms at interface through diffusion of Al into Fe, and the metallurgical bond is achieved.

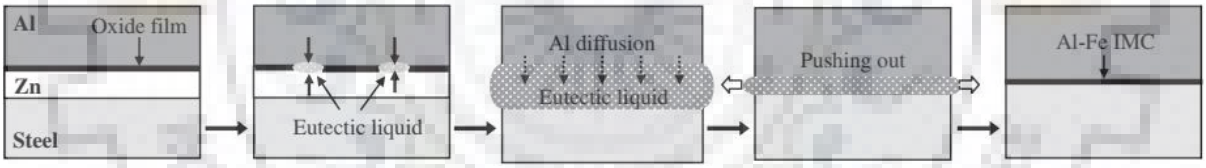

Fig. 22 Fluxing behaviour of Zn coating (Ueda et al., 2011) [11].

ii.) **Reducing IMC growth:** contact resistance is reduced by presence of Zn coating at joint interface, thus lowers the interfacial temperature. Further heat utilized for melting of remaining Zn coating at interface, lowers the actual heat input for reaction between Al and steel at the interface, which resulted in development of thinner but uniform IMC.

In 2011, Ueda et al. [11] welded Al alloy (6000 series) with Zn based coated steel in order to obtain higher joint strength in lower range of welding current and evaluated the effect of various Zn based coating (Al-Mg- Zn, Zn, Al- Zn) on the bond ability of steel/Al joints.

Following result have been noted from Fig. 23–

i.) Regardless of coating material nugget diameter has increased with increase of current. In the higher range of welding current, all joint shows same diameter except GI.

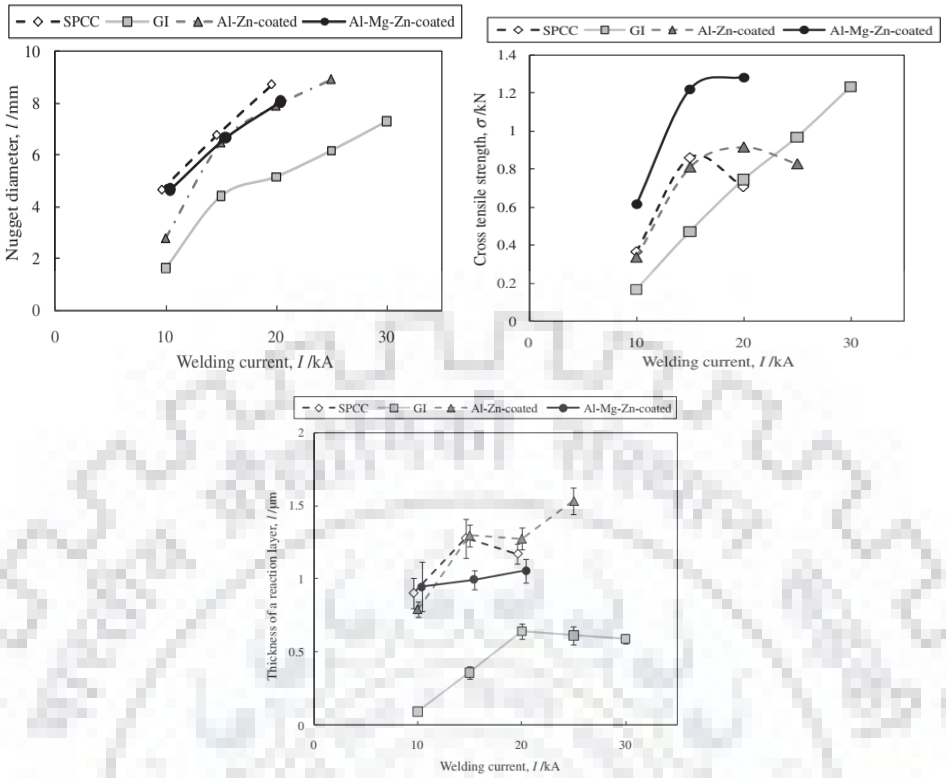

Fig. 23 Effect of welding current on (a) nugget diameter, (b) cross tensile strength, (c) thickness of reaction layer in Zn based coated steel/Al joints (Ueda et al., 2011) [11].

ii.) Al- Mg- Zn coating and Zn coating on GI reported thinner and regular reaction layer (IMC) due to fluxing action by low temperature eutectic reaction at the interface.

iii.) Thicker reaction layer with joints with SPCC and Al- Zn is due to fact that there is no coating on SPCC cause no reduction in resistance at interface (limited current carrying path) resulted in higher temperature at interface. In case of Al- Zn coating, there is already formation of IMC between steel and coating and melting point of reaction layer is higher than that of coating material. Thus, this reaction layer remains at the surface as coating material melts and did not allow the contact of newly surface of steel and Al, which is resulted in more thicker reaction layer at the interface.

iv.) Joint with Al- Mg- Zn coating leads the higher strength at lower welding current and almost constant for higher welding current due formation of sufficiently large nugget diameter, thinner and uniform reaction layer, and proper metallurgical bonding achieved at the interface.

v.) Joints with SPCC and Al- Zn coating shows sufficient high strength at lower welding current but suddenly decreases for higher welding current in spite of

increasing nugget diameter due to formation of thicker IMC and reduction in thickness of Al plate.

vi.) Joint with GI is reported-

Thinner, uniform, and regular reaction layer due to low temperature eutectic reaction.

Lower strength in lower current because there is no complete discharging of Zn coating and oxide layer at the lower current, which reduces contact resistance and thus, reduces effective heat input for reaction between steel and Al alloy, result smaller nugget diameter and hence lower strength in lower current.

Sufficient bonding and high strength in higher current because oxide film and Zn coating is completely discharged by eutectic reaction.

In 2011, Zhang et al. [10] performed RSW on dissimilar metals 6008 aluminium alloy and H220YD galvanised high strength steel. Following results have been concluded during study-

i.) Joint is composed of steel heat affected zone and molten Al alloy and it could be regarded as solid/liquid interface (joint by brazing mechanism), as shown in Fig. 7.

ii.) Al rich IMC is formed at the interface, which is consist of Fe_2Al_5 (tongue or lath like morphology) besides steel and Fe_4Al_{13} (needle like morphology) besides Al nugget. Thickest reaction layer measured at weld center, which comprised of 5µm lath like besides steel and long needle like phase with unequal thickness 2.5-8µm besides Al nugget i.e. maximum thickness of13µm is obtained.

iii.) Nugget diameter and welding strength is increases with increasing welding current as shown in Fig. 6 and 14. Maximum value of nugget diameter is 5.8mm at 9KA, 300ms and maximum tensile shear load recorded as 3309N at 9KA, 250ms.

iv.) Interfacial mode of failure is obtained in which crack is initiated (mainly in Fe_2Al_5 phase) and propagated though interfacial layer and partially through Al nugget, as shown in Fig. 18.

In 2016, Arghavani et al. [16] joined Al 5052 with galvanised steel and low carbon steel separately and investigated the role of Zn on microstructure and mechanical behaviour of joint. Following points are concluded-

i.) Intermetallic layer increases with increase of welding current for joint of Al/low carbon steel while its increases with increase of welding current till 12.0 kA and then decreases beyond it for Al/GI joint. However, thinner reaction layer is obtained for Al/GI joint for all range of current in comparison with Al/low carbon steel joint.

ii.) Presence of Zn coat on interface reduces electrical resistance and thus lower heat is generated. A part of generated heat is utilized for melting / vaporization of Zn coat in liquid metal, which reduces the effective heat for growth of reaction for Al/GI joint.

iii.) Increase tendency of IMC with increase of welding current is due to increase of heat input and compared to it, Zn latent heat for melting is negligible (101 kJ/kg). However, Zn evaporates at higher welding current (> 12 kA) and consumes more heat for evaporation (latent heat of evaporation 1782 kJ/kg), thus reduces the effective heat for intermetallic growth.

iv.) Incomplete joining of Al with GI due to inadequate heat generated is the reason for lower strength of joint Al/GI at low welding than joint Al/low carbon steel. However, with the increasing current joint becomes complete and continuous and strength increased. While at higher current (12 kA), reduction in intermetallic thickness and increment of nugget diameter is the reason for drastic improvement in tensile strength of Al/GI joint.

2.9.3 Effect of porosity/void on the performance of weld joint

In 1999, Gean et. al [16] studied the effect of discontinuity (porosity) on static and fatigue behaviour of resistance spot welded of 1.2 mm thick 5180- O Al alloy sheet. He concluded that

i.) Expulsion and porosity increase in nugget with increase in weld size and excessive porosity (up to 40 % of nugget diameter) do not affect static and fatigue and fatigue behavior of weld joint while maintaining a constant nugget diameter of 6.3mm.

ii.) Increase in electrode pressure increases the deep indentation. Thus, slightly reduce static performance (shear and cross tensile strength). But higher electrode force modified the edge of nugget, where fatigue crack initiate (residual stress at edge is modified and/or reduce the sharpness and stress concentration at notch). Thus, deep surface indentation at higher electrode force improved fatigue performance.

2.10 Gaps and Opportunities

Researchers have successfully welded steel with aluminium alloy by resistance spot weld. However, following gaps are identified:

i.) All joins of steel with aluminum alloy including joint of Zn coated steel and Al, has reported lower joint strength at lower current.

ii.) High IMC thickness is measured at low welding current and its increases with increasing current for all Al/steel joint, however, reduction in IMC thickness with increasing welding current at higher range of current is observed only for Zn coated steel/ Al joint.

iii.) Cover plate technique has not been used for RSW of Zn coated steel with Al alloy.

Thus, present work is planned to achieve defect free, lower thickness of IMC, and high strength of steel/Al joint at lower current. To achieve this objective Zn coated steel and Al alloy is welded by RSW with the use of cover plate technique.

2.11 Objective of present work

Overall work of present work is formulated as follows-

i.) Development of sound joint of aluminum and Zn coated steel by optimizing the process parameter and without the use of cover plate.

ii.) Development of sound joint of aluminum and Zn coated steel at previous optimized process parameter and with the use of cover plate.

iii.) Understanding the influence of welding current on intermetallic thickness, penetration, nugget diameter, and joint shear strength.

iv.) Studying the effect of cover plate on intermetallic thickness, electrode penetration, nugget diameter, and joint shear strength.

v.) Explore the effect of Zn coating on microstructure and mechanical behavior of RSW joint of aluminum and Zn coated steel.

vi.) Understanding the correlation of intermetallic layer, nugget diameter, defect, and joint strength.

vii.) Comparing and analyzing the joint properties for both joints - with and without cover plate.

Chapter 3

Experimental Materials and Procedure

3.1 Experimental Materials

In this experimental study, 1.5 mm thick Al 5052 - H32 alloy and 1.0 mm thick galvannealed steel were used as base metal (BM) and 1.0 mm thick cold rolled steel sheet (CRC- cold rolled & cooling) as a cover plate. Chemical compositions of material Al 5052 – H32 and steels are presented in Table 4 and Table 5.

Table 4

Chemical compositions of Al 5052 – H32

Material	**Si**	**Cu**	**Mn**	**Mg**	**Cr**	**Zn**	**Ni**	**Ti**	**Fe**	**Al**
Al 5052 – H32	0.049	0.006	0.016	2.629	0.196	0.009	0.004	0.016	0.186	Bal

Table 5

Chemical compositions of steels

Materials	C	Si	Mn	P	S	Al	Fe
Galvannealed Steel	0.0049	0.091	0.500	0.0189	0.0034	0.026	Bal
CRC Steel	0.07	0.067	0.18	0.013	0.01	0.051	Bal

3.2 Development of weld joint

i.) Al 5052 and galvannealed steel sheet machined into size of 100 × 25 mm [10] and CRC steel sheet is cut into 25 × 25 mm.

ii.) Before welding all the sheet were degreased with acetone, and then dissimilar metal lap joints were prepared as per configuration shown in Fig. 24 and 25. During welding Al sheet was placed on top of galvannealed steel sheet.

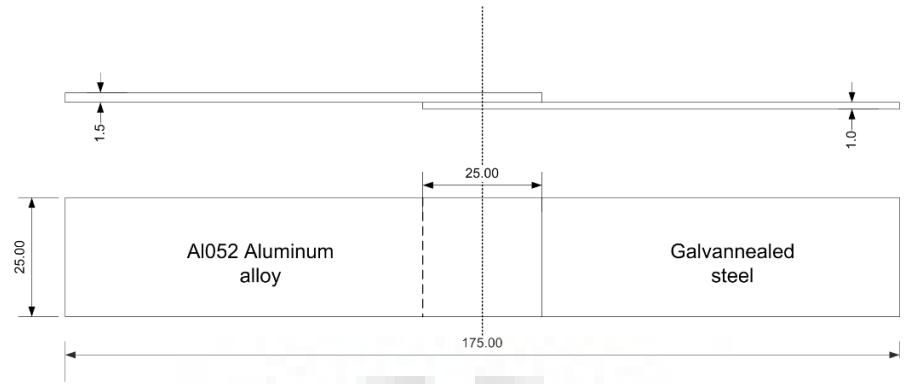

Fig. 24 Shape and size of specimen for joint without use of cover plate

To develop joint with cover plate, CRC steel was placed on Al sheet.

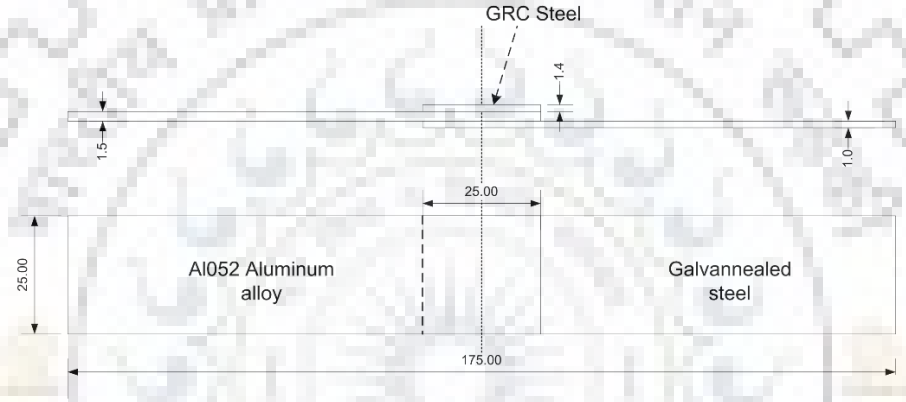

Fig. 25 Shape and size of specimen for joint with cover plate.

iii.) Welding is performed on resistance spot welding machine. Machine specification is given in Table 6.

Table 6

RSW machine specification

Capacity	150 KVA
Cooling	Water
Insulation	F Class
Supply	415V, 2 Phase Neutral
Resistance Weld Controller	Forwel AK – 54V
Mfg.	2009, The Saurabh Technologies Bhosari Pune

Fig. 26 Resistance spot welding machine.

iv.) Joints were developed as per welding condition presented in Table 7, in which welding current was changed every 0.5 kA between 7.0 kA and 12.0 kA at the fixed electrode pressure and welding time.

Table 7

Welding condition

Electrode specification	Cu- Cr alloy dome contours tip of electrode (Φ8)
Welding current	6.0, 7.0, 7.5, 8.0, 8.5. 9.0, 9.5, 10.0, 10.5,11.0 11.5, 12.0 kA
Welding time	0.94s (SC = 22, WC = 15, HC = 10)
Electrode pressure	6.4 kg/cm^2
Pre treatment	Degreased with acetone

v.) Three samples were welded for joint without cover plate and two samples were welded for joint with cover plate corresponding to each current between 7.0 kA and 12.0 kA with an increment of 0.5 kA. Few actual welded samples for both joint at different welding current are shown in Fig. 27 and 28.

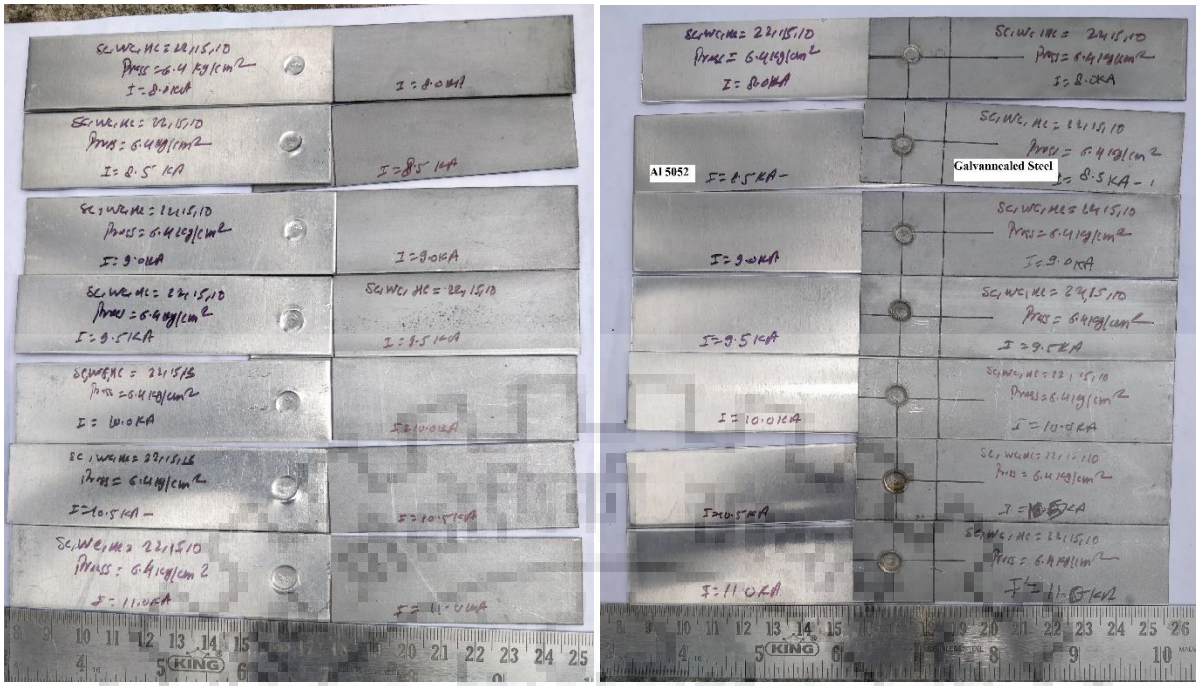

Fig. 27 Actual welded sample for joint without cover plate at welding current 8.0 kA to 11.0 kA with an increment of 0.5 kA.

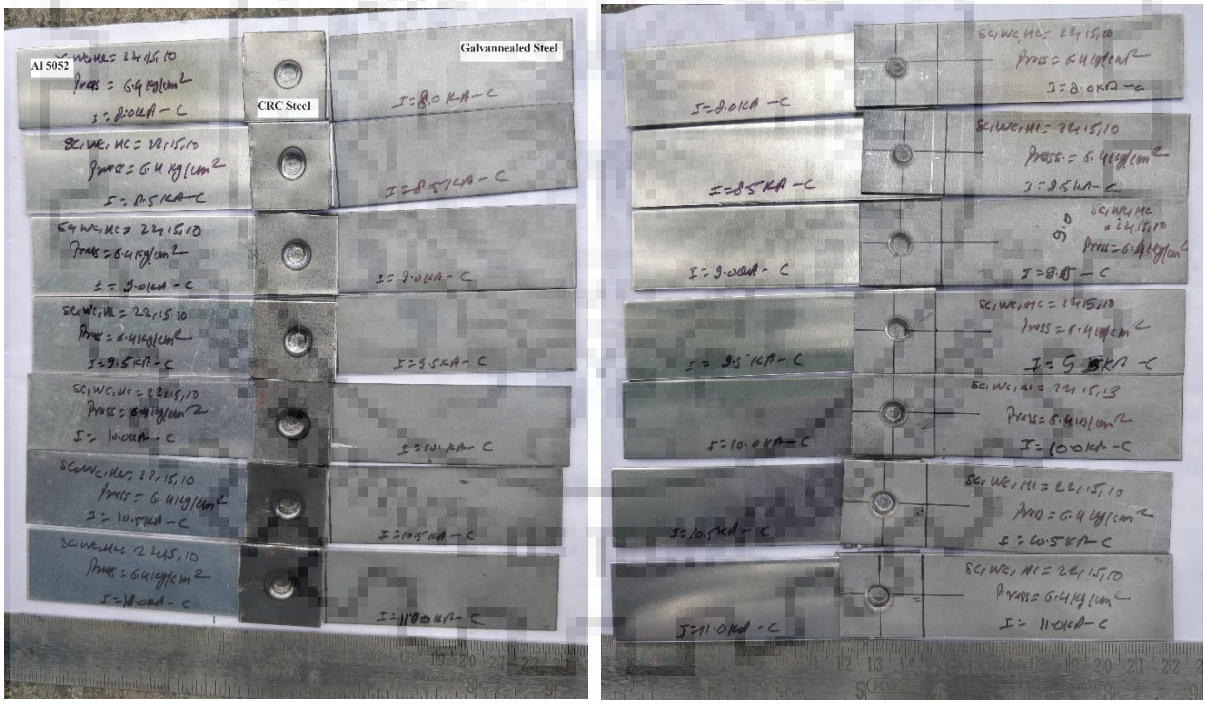

Fig. 28 Actual welded sample for joint with cover plate at welding current 8.0 kA to 11.0 kA with an increment of 0.5 kA.

3.3 Weld Characterization

3.3.1 Metallographic Examination

i.) Total sixteen sample were welded corresponding to welding current bewtween 8.0 kA to 11.0 kA with increment of 0.5 kA for both joint (8 for joint with cover plate and 8 for joint without cover plate, as displayed in Fig. 27 and 28. After welding, to obtained metallographic specimen for microstructure examination ,all the joints were cross sectioned through the weld nugget centre and perpendicular to surface plane.

ii.) Cross- sectioned specimen were polished with the help of emery paper to prepare the the surface free from umwanted material, and dirt and to make the sudface suitable for microstructure examination. Grit size used were (180, 320, 400, 600, 800, 1200, 1500, and 2000). After emery paper polishing, samples were polished with the help of aluminum oxide powder (alumina) over the cloth.

iii.) To study the carbon migration phenomenon, polished samples were etched with 3% Nital (100 ml ethanol + 3 ml nitric acid) for 15- 20sec.

iv.) Macroscopic examination of weld cross section were analyzed under stereo microscope (Make : Nikon SMZ 745T). All the macrograph were captured at 10X magnification.

v.) Microstructure and intermetallic layer were examined using otical microscope (Make: Leica DMi8 M) and field emission scanning electron micoscope (FE – SEM) (Make: Quanta 200F). Micrographs were captured at 1000X, 2500X, and 5000X magnification.

3.3.2 Mechanical property

Shear tensile tests of all welded sample were cariied out at universal testing machine (UTM) (Make: Instron 5980) with 100 KN axial load capacity at crosshead speed of 0.5 mm/min and at room temperature. Tensile load was evaluated by the average value of three specimen for joint without cover plate and by the average value of two specimen for joint with cover plate under the same welding condition.

Images of fractured surfaces were captured under stereo microscope (Make : Nikon SMZ 745T) at 10X magnification and nugget diameter was measured.

Chapter 4

Results and Discussion

4.1 RSW of Al 5052/galvannealed Steel – without use of cover plate

4.1.1 Microstructure evaluation of interface - macroscopic examination

Stereoscopic images of the cross section of welded joint under different welding current are shown in Fig. 29 (a -g). Aluminium plate is thinner at the weld centre (nugget) because Al alloy melts under applied current and squeezed near the periphery of nugget by electrode force. A dumbbell shaped cross section is observed at the weld cross section, in which thickness of Al plate decreases with increasing current i.e. indentation depth increases with increasing current. Since with increasing welding current, heat input at faying surfaces increases, resulted in more temperature and hence more molten Al alloy at weld centre.

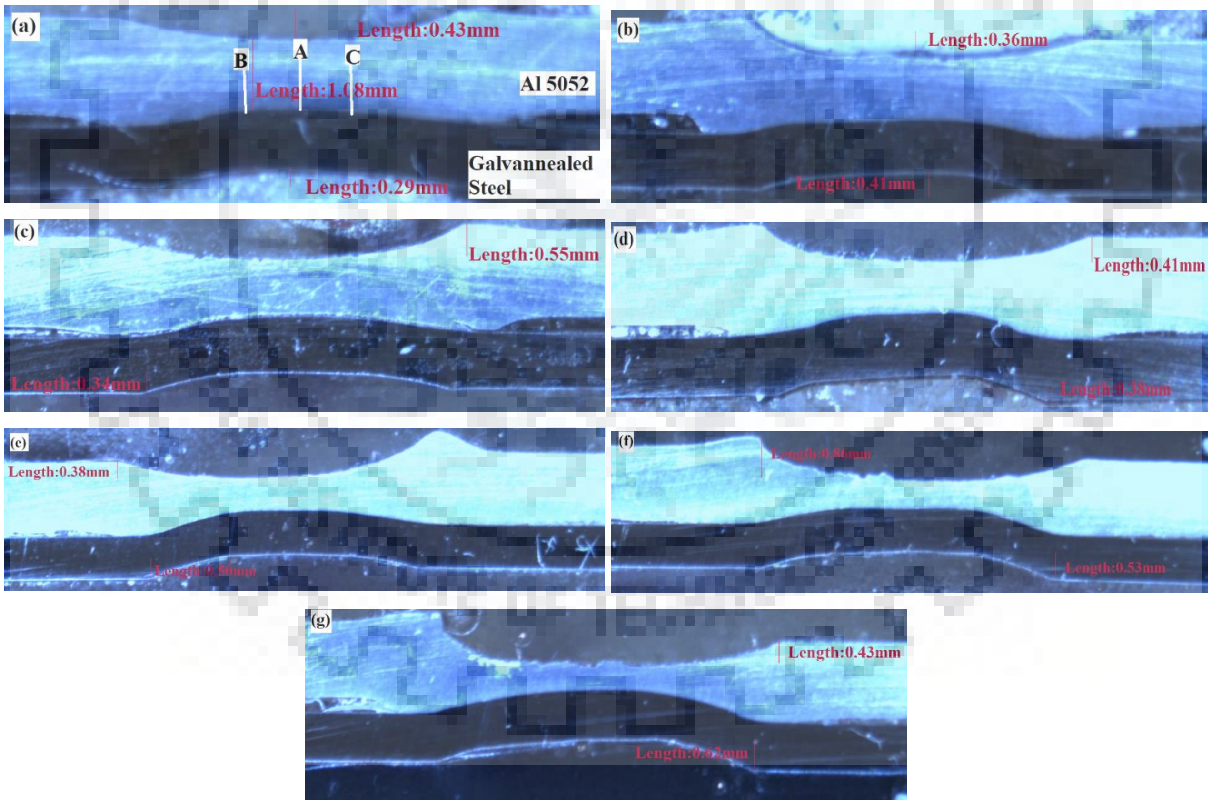

Fig. 29 Cross-section of welded joint at (a) 8.0 kA, (b) 8.5 kA, (c) 9.0 kA, (d) 9.5 kA, (e) 10.0 kA, (f) 10.5 kA, (g) 11.0 kA - (without cover plate).

4.1.2 Microstructure evaluation of interface - microscopic examination

4.1.2.1 Variation of reaction layer thickness

Optical images of interface region of joint A5052/galvannealed steel joint welded at the 8.5 kA is shown in Fig. 30 (a-c) and at 10.0 kA is shown in Fig. 31 (a-c). Images a to c is typical morphology corresponding to position A, B, C in Fig. 29 (a).

Interfacial reaction layer thickness depends on interfacial temperature and interaction time. Fig. 30 and 31 show that the reaction layer is regular and continuous, thicker at the central region and thickness decreases continuously with the distance from centre. Reason for this variation is temperature distribution in welded region, high temperature at central region and lower temperature near peripheral region due to heat loss.

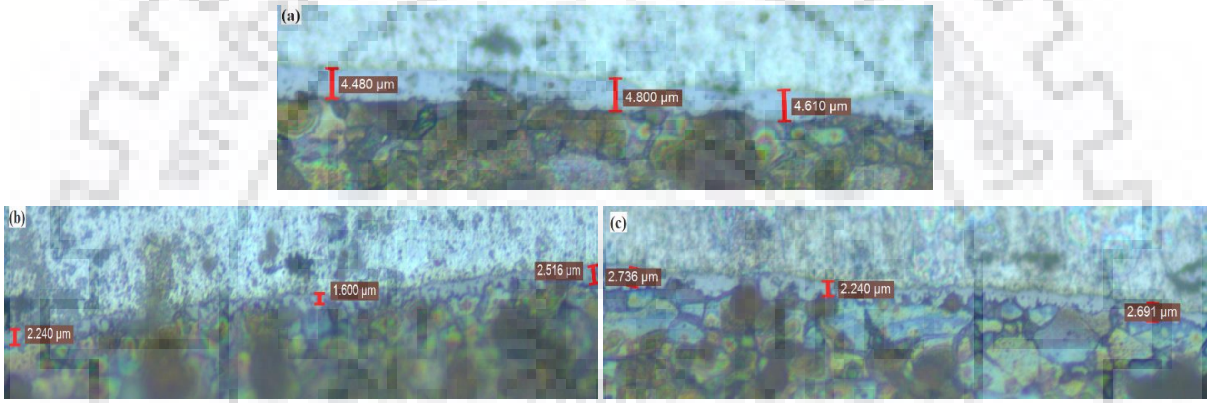

Fig. 30 Optical images of interface at 8.5 kA corresponding to location A, B, C in fig. 24 (a) - (without cover plate).

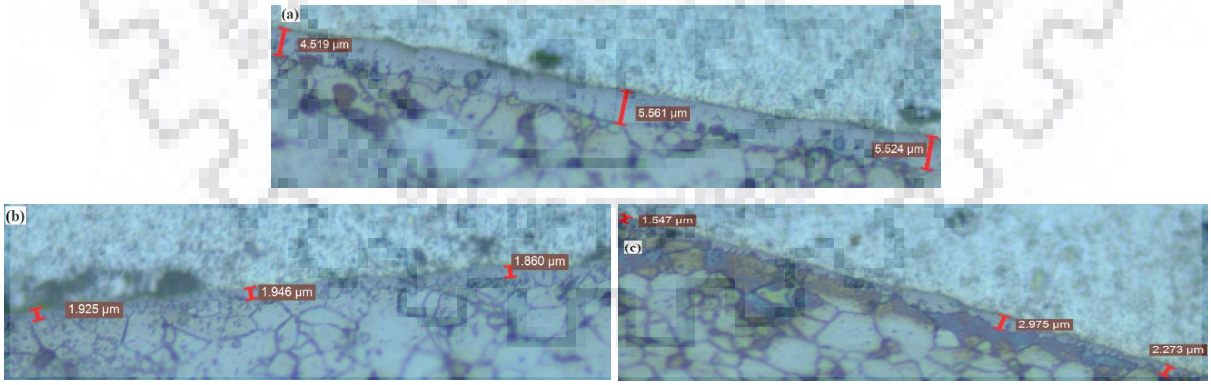

Fig. 31 Optical images of interface at 10 kA corresponding to location A, B, C in fig. 24 (a) - (without cover plate).

4.1.2.2 Effect of welding current on thickness of reaction layer

Fig. 32 express optical images of interface in central region at different welding current value corresponding to location A in Fig. 29 (a). At magnification of 20 µm images of interface at different current are captured and thickness of IMC is measured at three different location.

Average value of thickness at different welding current is presented in Table 8, and corresponding graph is plotted in Fig. 33.

Fig. 32 (a-g) shows that thinner and regular reaction layer is formed up to 10.0 kA current and it became irregular near steel side for higher current (≥ 10.5kA). Thinner reaction layer is achieved due to fluxing behaviour of Zn coating, achieved by eutectic reaction of Zn with the Al at lower temperature added with electrode force and resistance heating.

Electrode force and resistance heat generated on the faying surfaces deformed the oxide film from Al surface [10]. Zn coating reacts with Al at low temperature (melting point of Zn ~419 °C/ 693 K), and eutectic liquid of Al- Zn is formed thorough low temperature eutectic reaction, which is discharged at the periphery of nugget by electrode force. Thus, efficiently remove the oxide layer and leaves the clean, contaminated free surface, and ensured good wettability which enables more uniform growth of reaction layer through diffusion of Al and steel [9, 10]. Since oxide layer and Zn coating were not completely discharged at lower range of current [10]. Presence of Zn coating lowers the contact resistance, therefore lower heat is generated and Zn coating consumes part of generated heat for melting at lower temperature and evaporation at higher temperature (latent heat is consumed as a part of generated heat), which reduces the actual heat input available for growth of interfacial reaction , resulted in formation of thinner IMC at the joint interface[9, 15].

Fig. 33 shows effect of welding current on thickness of intermetallic layer, in which average reaction layer thickness varies between 4.099 µm and 5.201 µm. In the joint of Al 5052 alloy and Zn coated galvannealed steel, reaction layer thickness increases slightly with increment of welding current up to 10 kA, since heat input at weld interface have direct relationship with welding current. However, thickness of reaction layer decreases for welding current > 10 kA.

Increment in welding current up to 10 kA leads to increase in effective heat available for reaction at interface. At low welding currents, Zn coating melted (mostly latent heat is consumed as a part of generated heat) and it is negligible compare with increment in generated heat. Thus, growth of intermetallic layer.

For higher welding currents (> 10 kA), there is vaporisation of Zn coat. Latent heat of Zn vaporisation (~1782 kJ/kg) is much higher than melting (~101 kJ/kg). Thus, evaporation consume more generated heat than melting, therefore effective heat available for interfacial reaction is reduced and thickness of reaction layer is reduced for welding current beyond 10 kA as shown in Fig. 33.

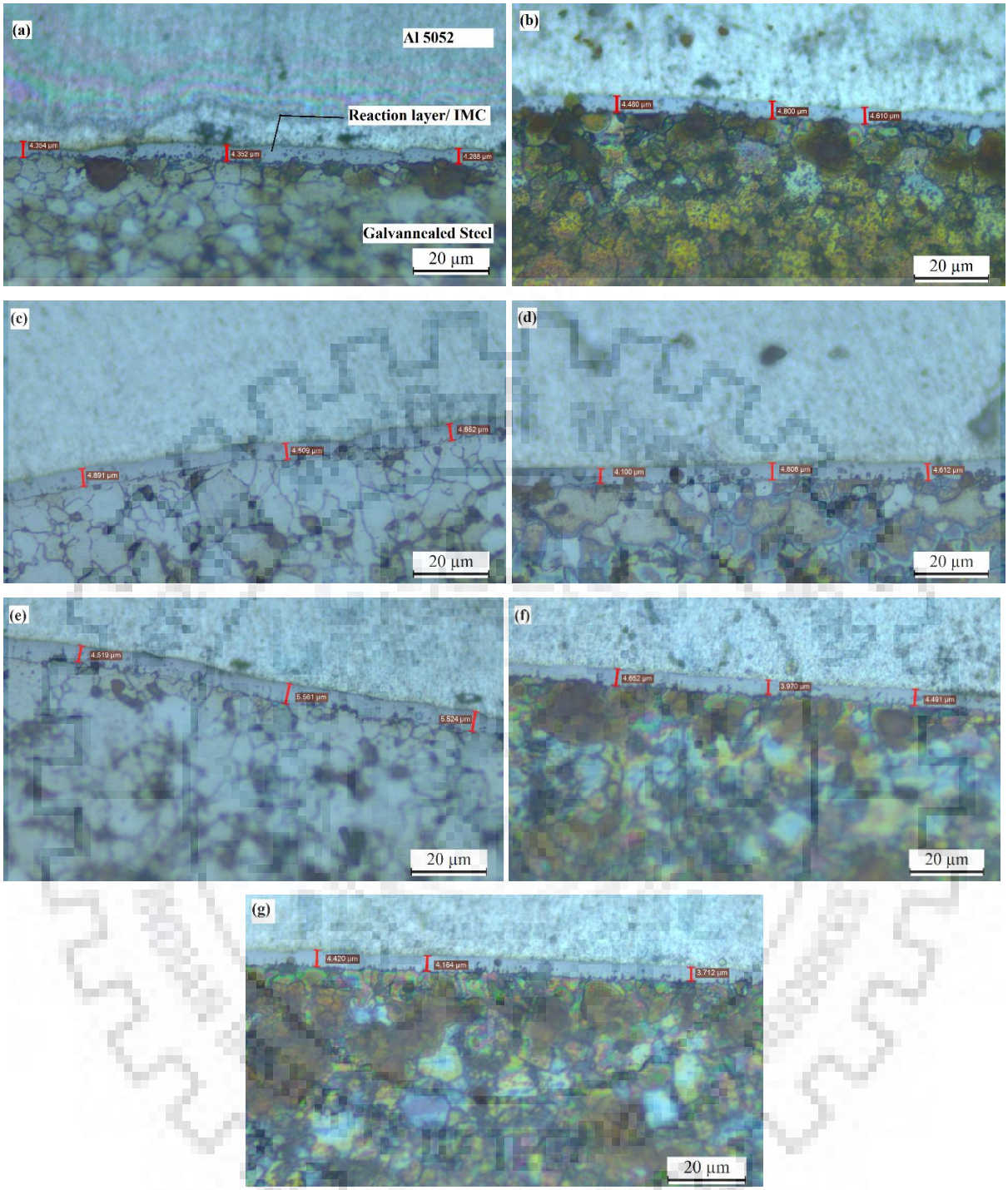

Fig. 32 Optical images of the joint interface in central region at (a) 8.0 kA, (b) 8.5 kA, (c) 9.0 kA, (d) 9.5 kA, (e) 10.0 kA, (f) 10.5 kA, (g) 11.0kA - (without cover plate).

Table 8

Effect of welding current on thickness of IMCs (Central region- without cover plate)

Welding Current (kA)	Thickness of Reaction Layers (Central Region – Without Cover Plate) (µm)			Average Thickness of Reaction layer (Central Region- Without Cover Plate) (µm)
8.0	4.352	4.352	4.288	4.330
8.5	4.480	4.800	4.610	4.630
9.0	4.891	4.509	4.652	4.684
9.5	4.100	4.608	4.612	4.440
10.0	4.519	5.561	5.524	5.201
10.5	4.652	3.970	4.491	4.371
11.0	4.420	4.164	3.712	4.099

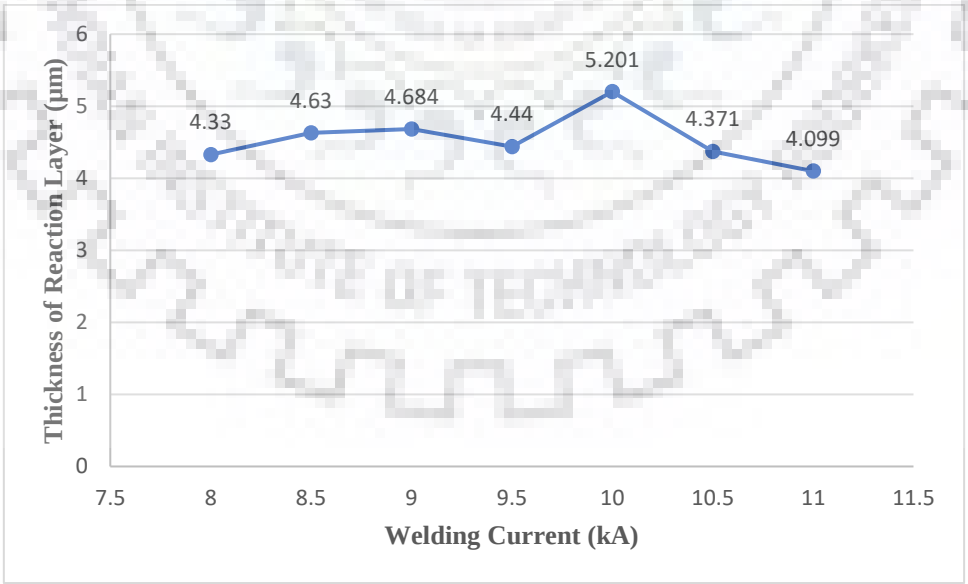

Fig. 33 Effect of welding current on thickness of reaction layer (central region – without cover plate).

4.1.3 Evaluation of joint properties

4.1.3.1 Effect of welding current on nugget diameter

Fig. 34 (a-j) express the stereoscopic images of fracture surface at different welding current. Aluminium metal expulsion begins at 9.0 kA as indicated in Fig. 34 (e) and increased with increasing current. Excessive weld metal expulsion is detected beyond 10.5 kA.

Nugget diameter is measured from fractured surface of sample failed in shear tensile test as expressed in Fig. 34 (a-j).

Measured value of nugget diameter at different welding current is presented in Table 9, and graph is plotted between average nugget diameter and welding current, as expressed in Fig. 35.

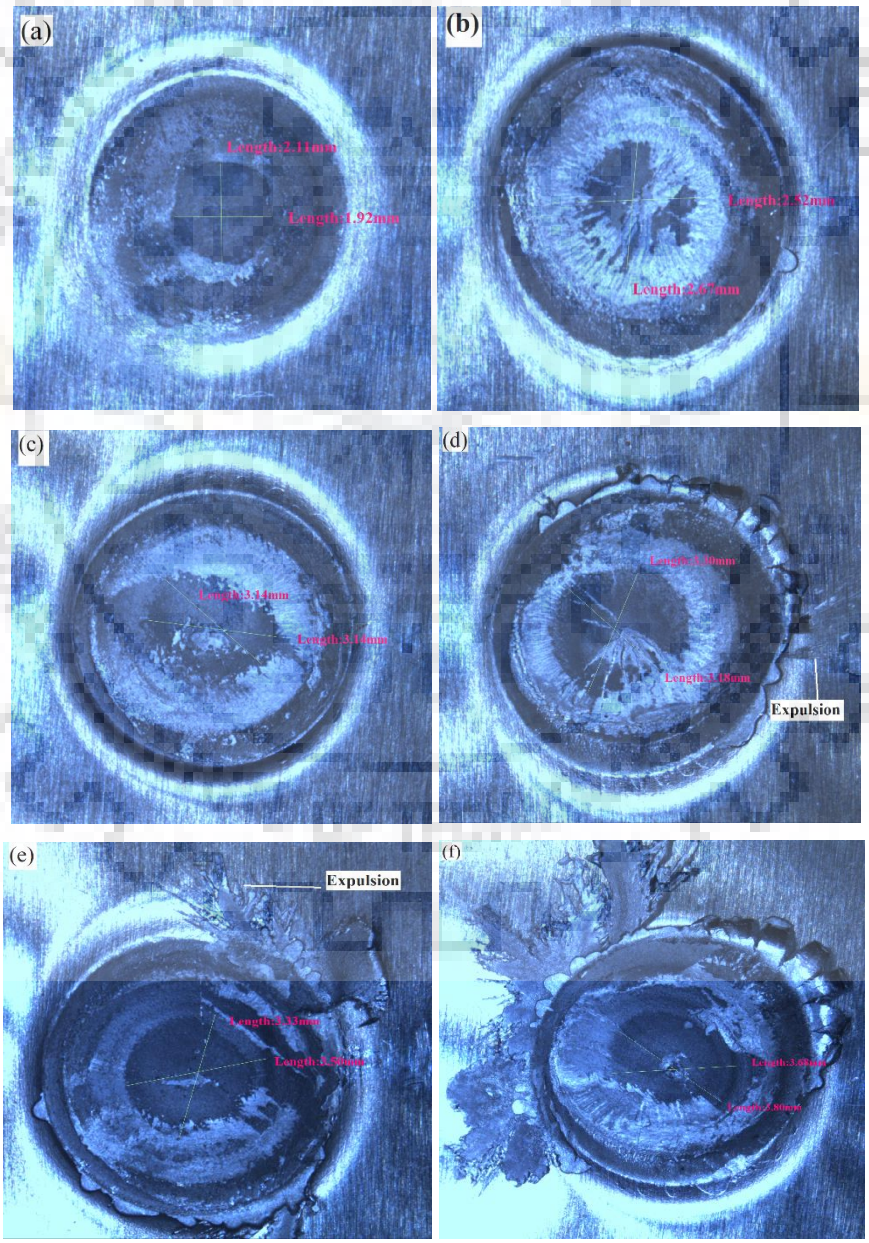

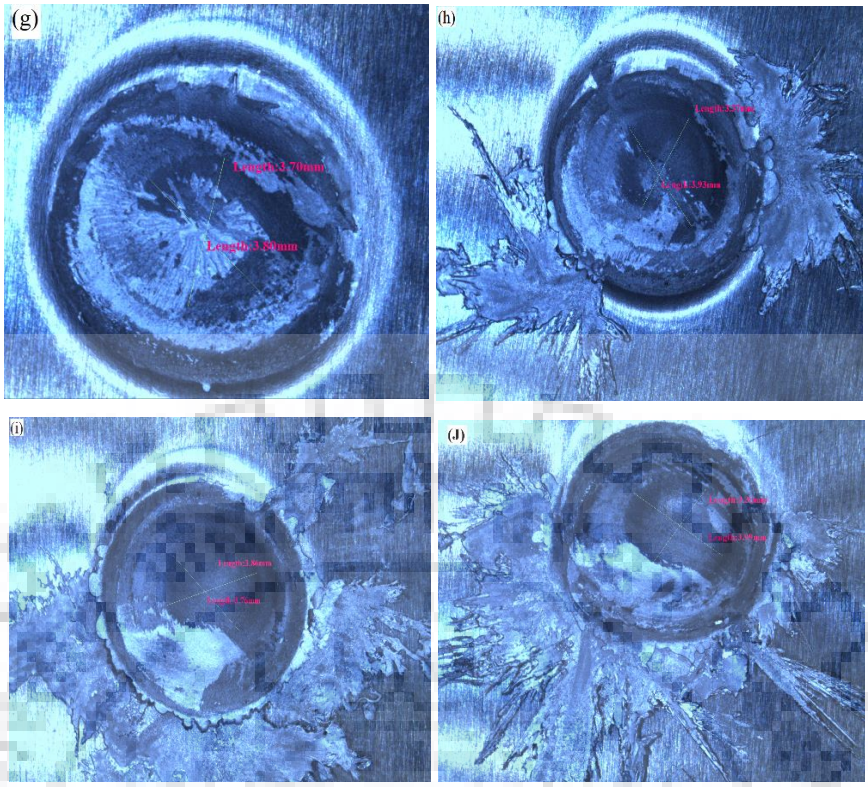

Fig. 34 Fracture surface at (a) 6 kA, (b) 7 kA, (c) 8 kA, (d) 8.5 kA, (e) 9.0 kA, (f) 9.5 kA, (g) 10 kA, (h) 10.5 kA, (i) 11 kA, (j) 11.5 kA - (without cover plate).

Melted nugget volume is a function of heat input at faying surface. Increasing welding cuurent increased heat input, which result in more melted volume. Thus, increase in nugget diameter. However, growth rate of nugget diameter is not contstant for all current value as shown in Fig. 35. Nugget diameter increases rapidly up to 8.5 kA, followed by slow growth of nugget upto 9.5 kA, and its almost constant for current beyond 9.5 kA. Average value nugget diameter is 3.74 mm at 9.5 kA and 3.75 mm at 10.0 kA.

Gradual change of nugget diameter beyond 9.5 kA , attributed to equilibrium between heat input at interface and heat loss to the surrounding.

Two parameters govern the growth rate of nugget [6] –

i.) Increase in electrical resistance due to temperature increase in weld nugget

ii.) Reduction in electrical resistance due to increment of nugget size

At early stage, welding heat (due to increase in welding current /time) has more pronounce effect because of small size of nugget. As the nugget size increases, it reduces the electrical resistance which limits the growth rate of nugget. Therefore, nugget size remains almost constant for high welding current/time.

Table 9

Effect of welding current on nugget diameter - (without cover plate)

Welding Current (kA)	Nugget Diameter (mm)		Average Nugget Diameter (mm)
6.0	2.11	1.92	2.02
7.0	2.52	2.67	2.60
8.0	3.14	3.14	3.14
8.5	3.30	3.18	3.24
9.0	3.33	3.50	3.42
9.5	3.68	3.80	3.74
10.0	3.70	3.80	3.75
10.5	3.37	3.93	3.65
11.0	3.86	3.76	3.81
11.5	3.30	3.99	3.65

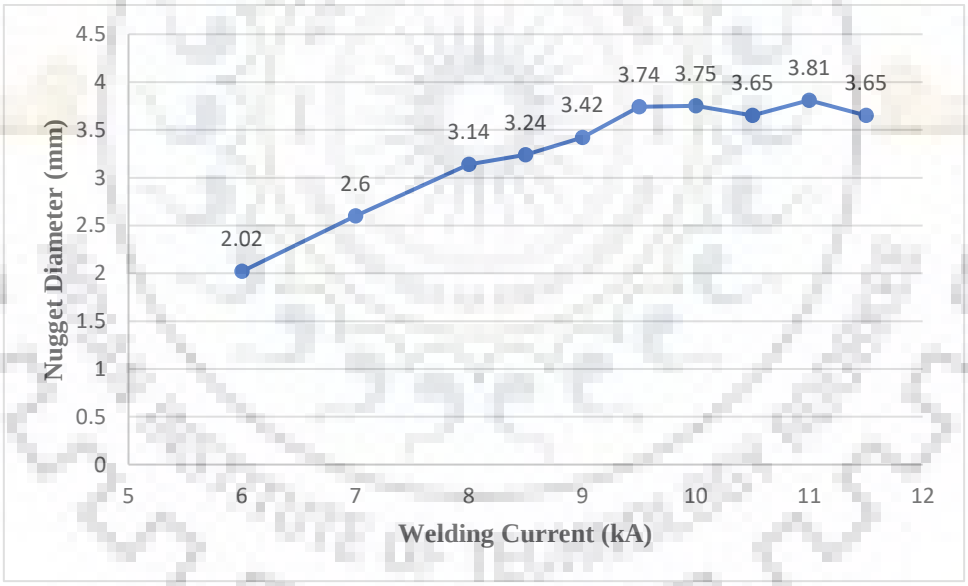

Fig. 35 Effect of welding current on nugget diameter - (without cover plate).

Fig. 36 (a-d) shows joint interface for higher current (≥ 9.5 kA) for which excessive metal explusion is reported in Fig. 34. With increasing current, nugget internal forces (due metal melting and expansion) exceeds electrode force and expulsion occurs. Expulsion reduces volume of melted nugget, which cause shrinkage and porosity formation, and crack in the IMC, and adcent to IMC in base metals during solidification, as it can be seen in Fig. 36. Thus,

excessive current will not increase nugget diameter but will create undesirable features (pores, shrinkage, cracks) which affectts the weld strength.

Fig. 36 indicates that undesirable feature like porosity, cracks in IMC and adcent to IMC in base metal increased with increasing current and IMC morphology became irregular adcente to steel side for current higher current (≥ 10.5 kA). Reason for this undesirable features at interace, is excessive weld metal expulsion and Zn coating evaporisation for higher current (≥ 10.5 kA), as exposed in Fig. 34.

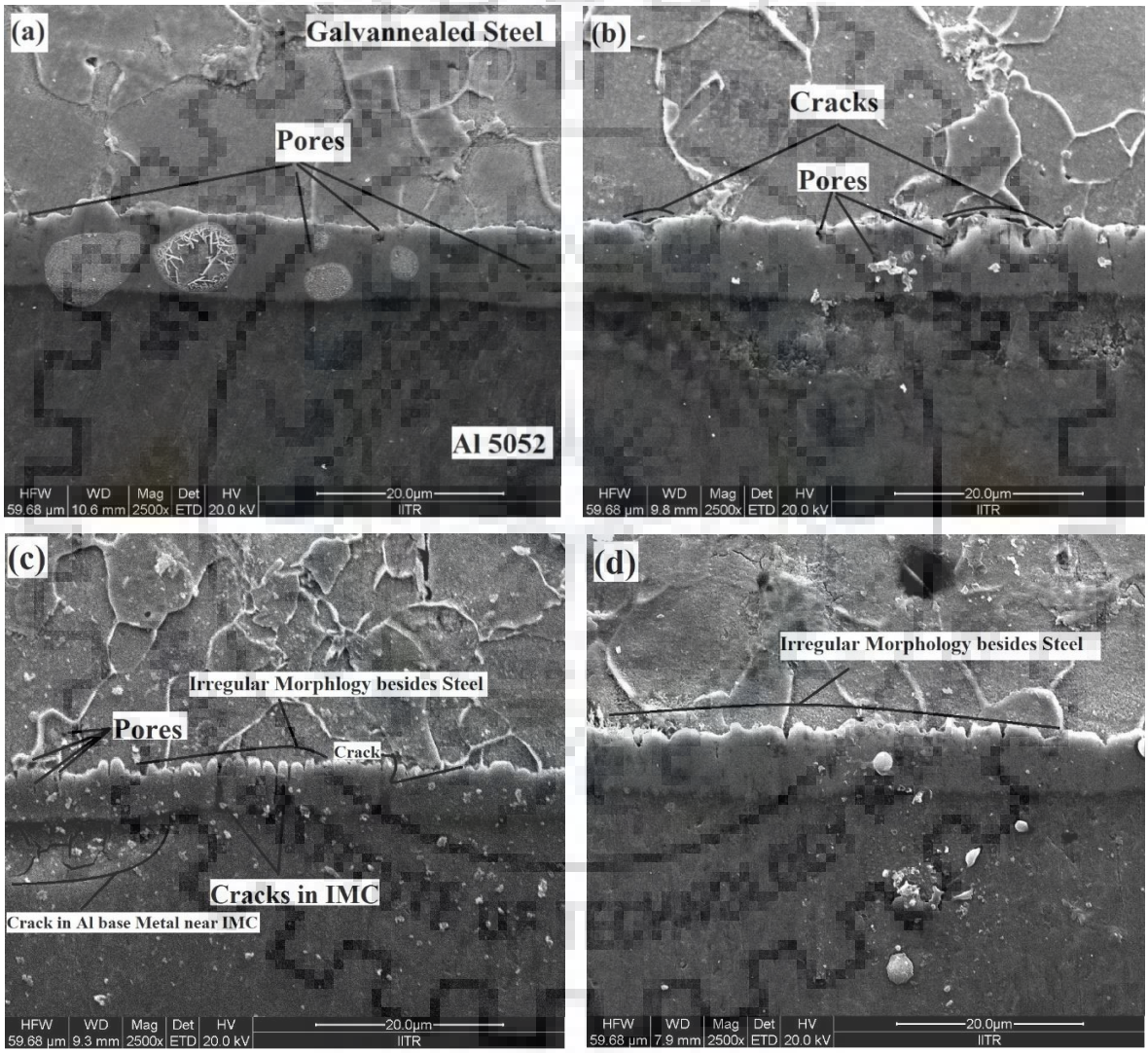

Fig. 36 SEM images of joint interface at (a) 9.5 Ka, (b) 10.0 kA, (c) 10.5 kA, (d)11.0 kA - (without cover plate).

4.1.3.2 Effect of welding current on joint thickness reduction

Electrode surface deep indentation at different welding current is measured from Fig. 29 and measured value of thickness reduction and % change in thickness reduction is presented in Table 10 and corresponding graph is presented in Fig. 37.

Fig. 37 shows that % thickness reduction increases linearly with increasing current. This behaviour of varying indentation depth under different welding current is due change of heat input at interface. Increase of welding current resulted in more heat input at faying surface and thus, more molten metal at joint interface, resulted in increase of electrode indentation under applied electrode force.

Table 10

Effect of welding current on joint thickness reduction - (without cover plate)

Welding Current (kA)	Total Thickness of Joint at Nugget Centre before Welding (mm) – X	Total Thickness Reduction at Nugget Centre after Welding (mm) – Y	Thickness Reduction (%) = Y/X * 100
8.0	2.5	0.56	22.4
8.5	2.5	0.63	25.2
9.0	2.5	0.74	29.6
9.5	2.5	0.79	31.6
10.0	2.5	0.88	35.2
10.5	2.5	0.96	38.4
11.0	2.5	1.05	42.0

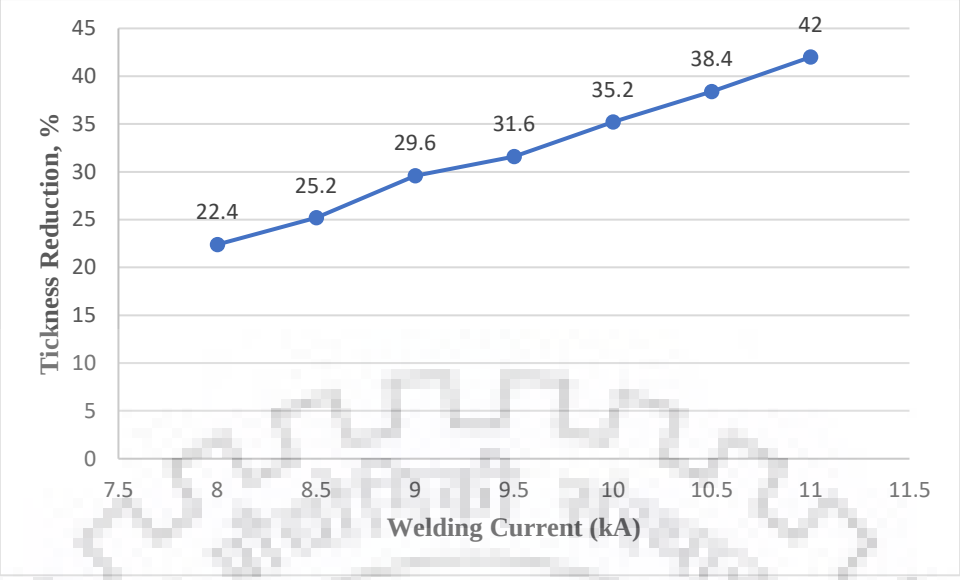

Fig. 37 Effect of welding current on joint thickness reduction - (without cover plate).

4.1.3.3 Effect of welding current on shear strength of joints

Three samples are being tested on UTM corresponding to each current. Failure load is noted from load- extension curve as represented in Annexure A and values are presented in Table 11. Similarly, variation of average shear strength with increasing current is plotted in Fig. 38. Results indicates that slope of shear load vs current is not constant for all current. It's increased in a quasi- linear characteristic up to 9.5kA, beyond 9.5 kA joint load have slow growth till 11kA, and slowly decreased for higher current (≥ 11.5kA). Highest joint shear strength is 4049.3N at 11.0kA and joint strength 3915 N is at 9.5kA.

Since joint strength is dependent on bonding zone length (nugget diameter), formation of intermetallic compound and weld defect (pores/void, cracks) present at joint interface, and electrode indentation. However, Gean et al. [16] reported that porosity (upto 40% of nugget diameter) in weld nugget does not affect static performance of resitance spot weld of aluminum alloy. In this study, therefore, porosity formed in aluminium nugget would not have much affect on joint strength and slow growth of tensile shear load is in good accordance with change in nugget diameter and reaction layer thickness with increasing current up to 11.0 kA as shown in Fig. 33 & 35. Excessive sheet thickness reduction, expulsion, and thus reduced nugget diameter could be the possible reason for strength reduction for current beyond 11.0 kA.

Table 11

Effect of welding current on joint shear load – (without cover plate).

Welding Current (kA)	Tensile Shear Load (N)			Average Tensile Shear Load (N)
	Sample 1	Sample 2	Sample 3	
7.0	1969	1931	2144	2014.7
8.0	2943	2817	3130	2963.3
8.5	3460	2988	3377	3275.0
9.0	3245	3537	3415	3399.0
9.5	4075	3923	3747	3915.0
10.0	3776	3705	4080	3853.7
10.5	3646	4125	3589	3786.3
11.0	3866	4067	4215	4049.3
11.5	3778	3625	3236	3546.3
12.0	4001	3234	2841	3358.7

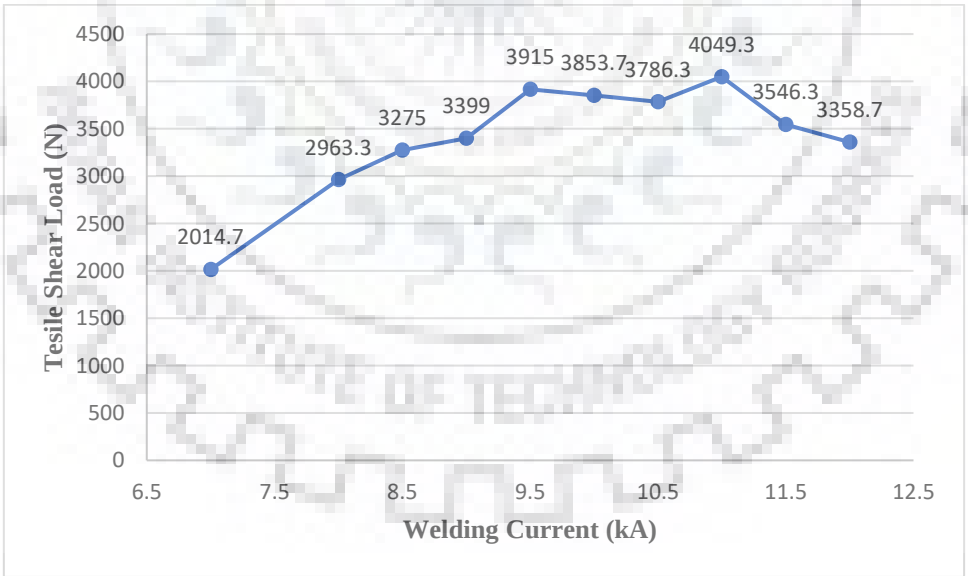

Fig. 38 Effect of welding current on joint shear load – (without cover plate).

4.2 RSW of Al 5052/galvannealed Steel – with the use of cover plate

Following result is concluded from study of Al5052/galvannealed steel joint without cover plate-

i.) At lower current, lower joint strength due to low interfacial temperature for bonding formation and hence lower bonding zone (nugget diameter) is achieved because of lower effective heat available for bonding. Lower effective is due to low heat generation at interface coupled with heat loss to the electrode and surrounding because of high thermal conductivity of Al. But at higher current, interfacial temperature is increased by increased heat input, which enlarges bonding zone resulted in improved strength.

ii.) Interfacial reaction layer thickness reduced and bonding zone length (nugget diameter) increased for higher current (10.5 kA, and 11.0 kA), which improved joint shear strength.

iii.) Excessive current cause undesirable feature in the joint like expulsion, shrinkage, porosity, cracks, high seat thickness reduction (electrode indentation), and electrode degradation.

Favourable joint property i.e. lower reaction layer thickness, large bonding zone (nugget diameter), which is achieved at higher current for without cover plate, along with minimum electrode indentation and degradation could also be achieved at lower temperature, by controlling heat loss to the electrode and directed heat toward joint interface. And this favourable joint property at relatively lower temperature is achieved by use of cover plate technique.

In this technique, cover plate is placed on Al sheet, which have relatively low electrical and thermal conductivity than aluminium alloy, so the higher heat generated in cover plate is directed towards aluminium/steel interface resulting an increase of interface temperature. Thus, improved nugget diameter, and reduced reaction layer and hence improved joint strength.

Considering low cost and availability, cold rolled steel sheet (CRC) of thickness 1 mm is used as cover plate.

4.2.1 Microstructure evaluation of interface - macroscopic examination

Fig. 39 (a-g) is the stereoscopic images of the cross section of welded joint under different welding current. Aluminium plate is thinner at the weld centre (nugget) because Al alloy melts under applied current and squeezed near the periphery of nugget by electrode force. A dumbbell shaped cross section is observed at the weld cross section, in which thickness of Al plate decreases with increasing current (up to 10 kA). Aluminium is completely squeezed out at higher current i.e. at welding current 10.5 kA and 11.0 kA. Depth of indentation also increases with increasing current. Since with increasing welding current, heat input at faying surfaces increases, resulted in more temperature and hence more molten Al alloy at weld centre. Gas porosities are also visible in Al alloy at the weld centre as revealed in Fig. 40.

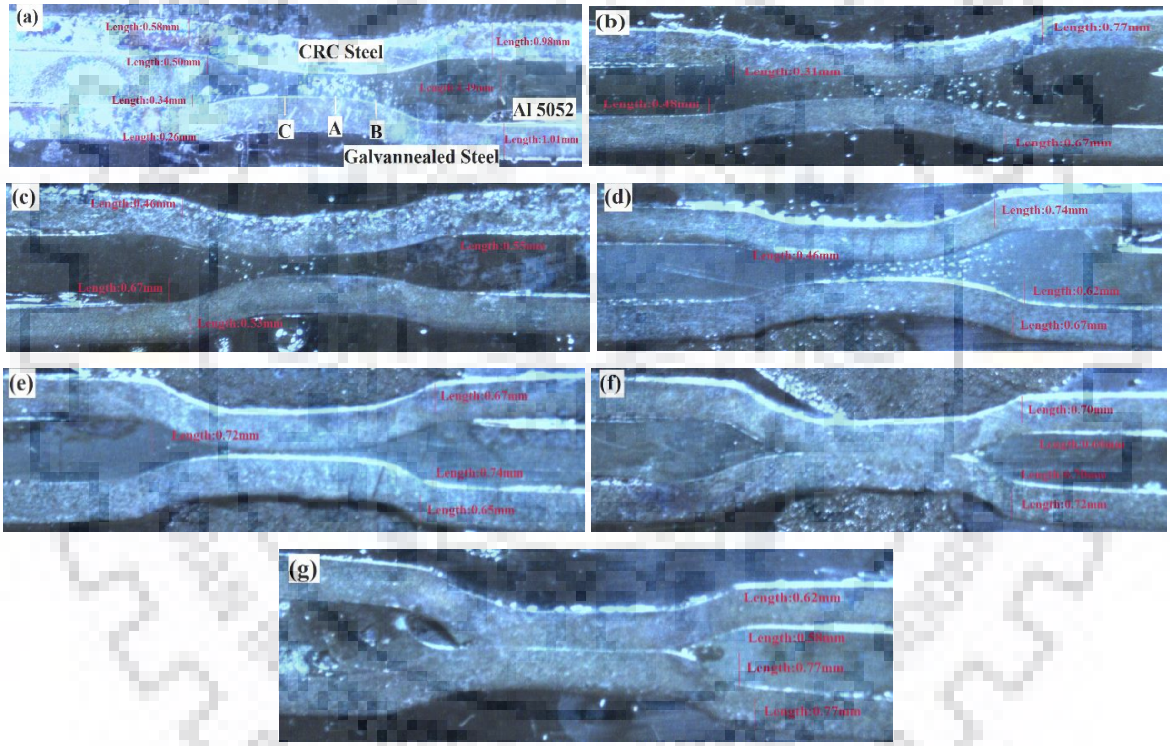

Fig. 39 Cross-section of welded joint at (a) 8.0 kA, (b) 8.5 kA, (c) 9.0 kA, (d) 9.5 kA, (e) 10.0 kA, (f) 10.5 kA, (g) 11.0 kA – (with cover plate)

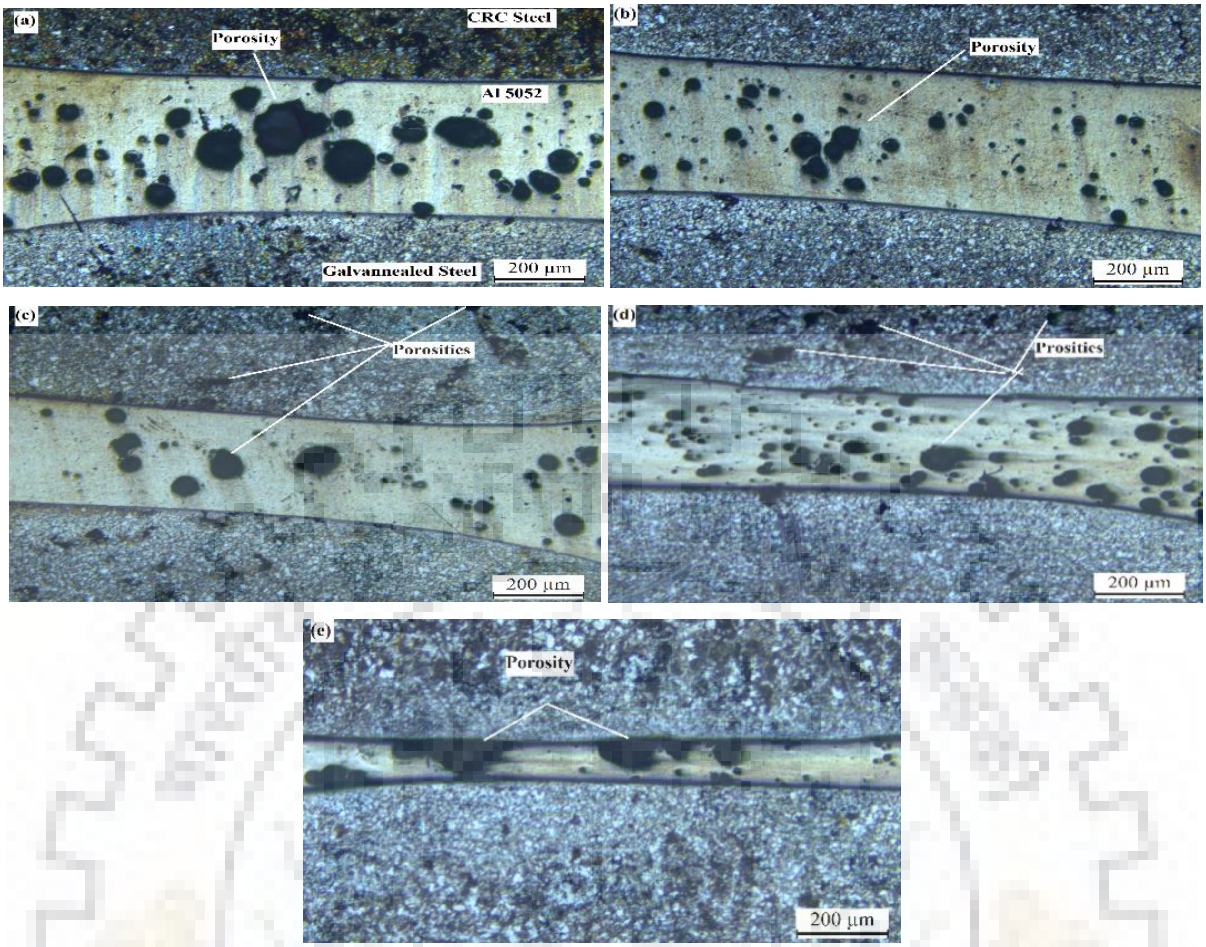

Fig. 40 Optical image of weld cross- section in central region at (a) 8.0 kA, (b) 8.5 kA, (c) 9.0 kA, (d) 9.5 kA, (e) 10.0 kA – (with cover plate).

4.2.2 Microstructure evaluation of interface - Microscopic Examination

4.2.2.1 Variation of Reaction Layer Thickness

Optical images of interface region of joint A5052/galvannealed steel joint welded at 8.0 kA is shown in Fig. 41 (a-c) and at 9.0 kA is shown in Fig. 42 (a-c). Images a to c is typical morphology corresponding to position A, B, C in Fig. 39 (a).

Interfacial reaction layer thickness depends on interfacial temperature and interaction time. Fig. 42 and 43 revealed that the reaction layer is regular and continuous, thicker at the central region and thickness decreases continuously with the distance from centre. Reason for this variation is temperature distribution in welded region, high temperature at central region and lower temperature near peripheral region due to heat loss.

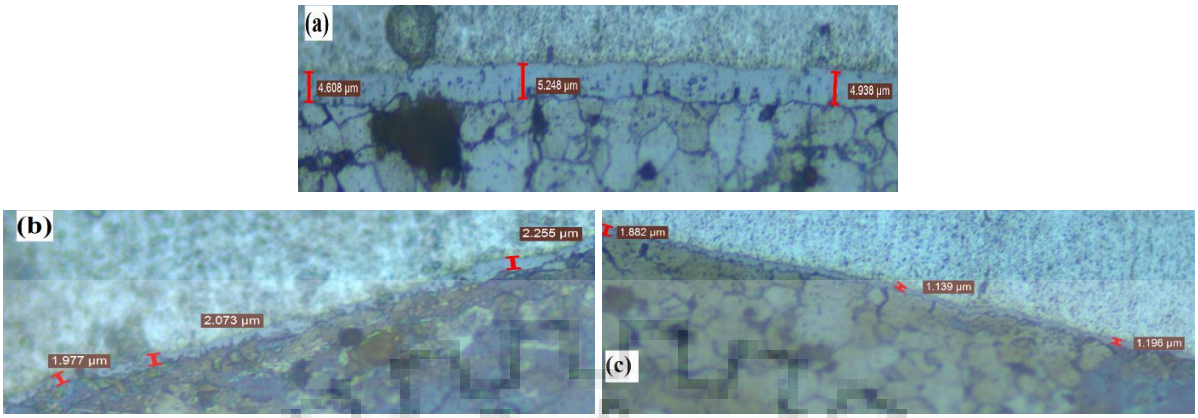

Fig. 41 Optical images of interface at 8.0 kA corresponding to location A, B, C in fig. 35 (a) - (with cover plate).

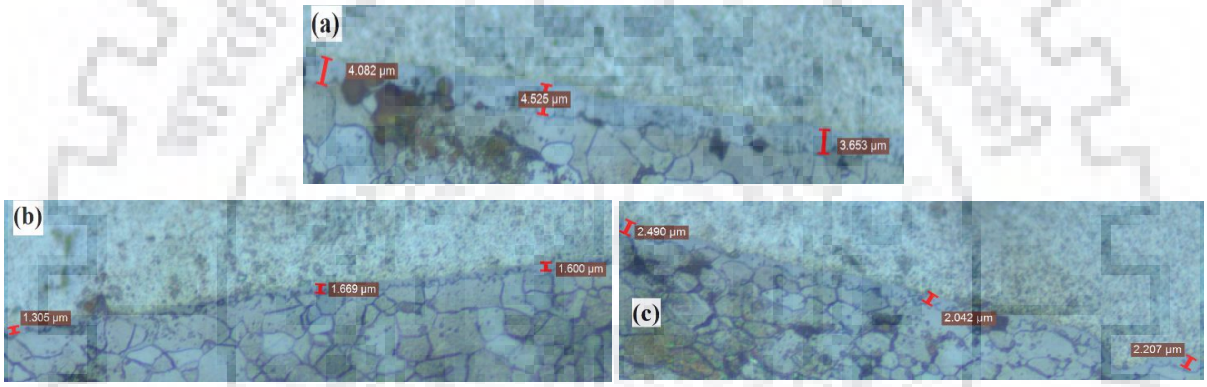

Fig. 42 Optical images of interface at 9.0 kA corresponding to location A, B, C in fig. 35 (a) - (with cover plate).

4.2.2.2 Effect of welding current on thickness of reaction layer

Fig. 43 (a-g) express the optical images of interface in central region at different welding current value corresponding to location A in Fig. 39 (a). Since there is no reaction layer for current beyond 10.0 kA as detected in Fig. 39 (f) & (g), so analysis for intermetallic thickness is limited up to 10.0 kA. At magnification of 20 µm images of interface at different current are captured and thickness of IMC is measured at three different location. Average value of thickness at different welding current up to 10.0 kA is presented in Table 12, and corresponding graph is plotted in Fig. 43 (a-g).

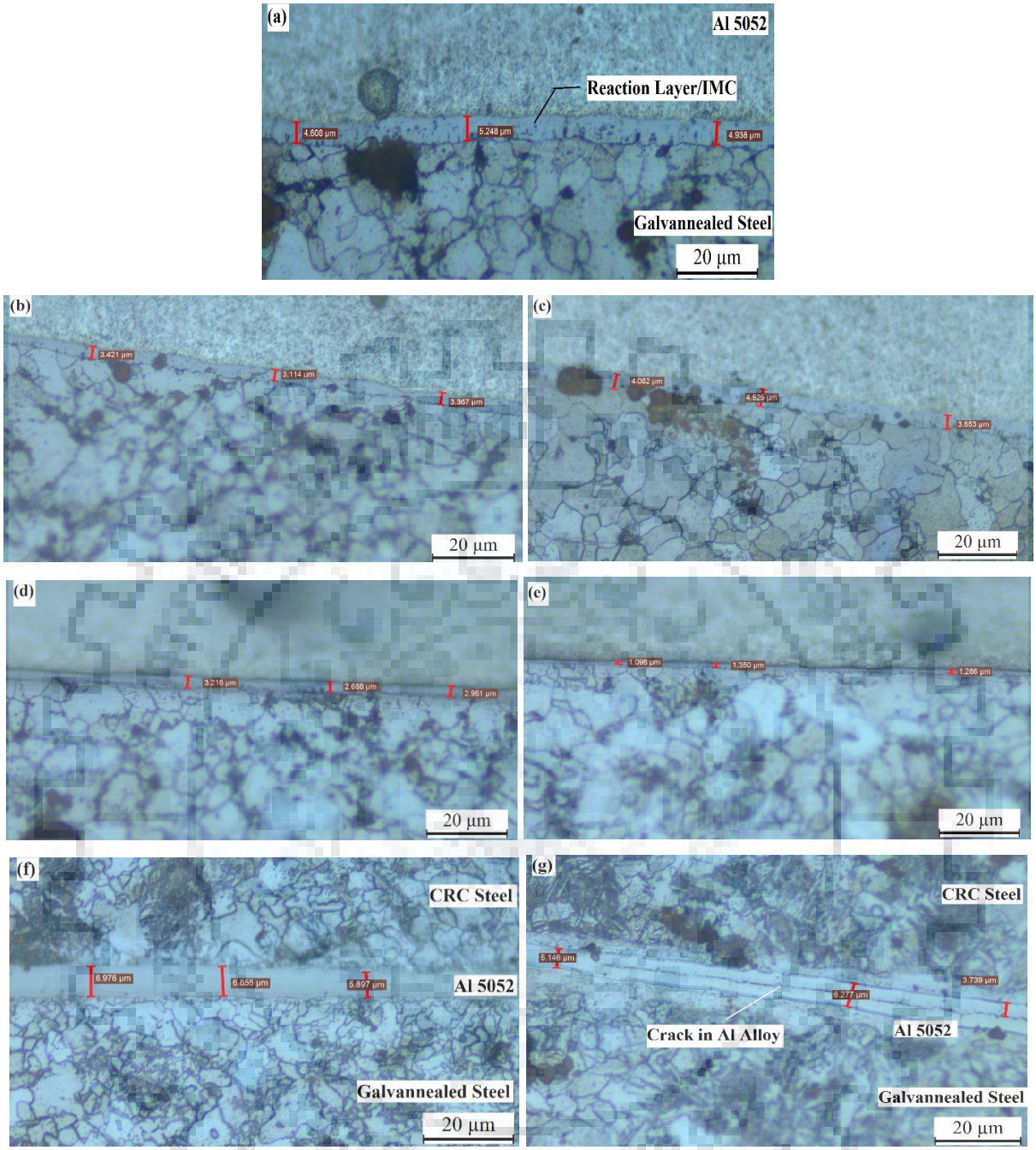

Fig. 43 Optical images of the joint interface in central region at (a) 8.0 kA, (b) 8.5 kA, (c) 9.0 kA, (d) 9.5 kA, (e) 10.0 kA, (f) 10.5 kA, (g) 11.0kA - (with cover plate).

Fig. 43 indicate that thinner and uniform reaction layer is formed up to 10 kA current. Thinner reaction layer is achieved due to fluxing behaviour of Zn coating, achieved by lower temperature eutectic reaction of Zn with the Al added with electrode force and resistance heating.

Electrode force and resistance heat generated on the faying surfaces deformed the oxide film on Al surface [10]. Zn coating reacts with Al (melting point of Zn ~419 °C/ 693 K), and eutectic liquid of Al- Zn is formed through low temperature eutectic reaction, which is discharged at

the periphery of nugget by electrode force. Thus, efficiently remove the oxide layer and leaves the clean, contaminated free surface, and ensured good wettability which enables more uniform growth of reaction layer through diffusion of Al and steel [9, 10].

Significant amount of Zn coating is melted and reacts with oxide film on Al through and formed eutectic liquid through low temperature eutectic reaction, which is squeezed out by electrode force. However, few Zn coat present in liquid phase at interface, which lowers the contact resistance, therefore lower heat is generated and Zn coating consumes part of generated heat for evaporation at higher temperature (latent heat is consumed as a part of generated heat). Thus, effective heat available for growth of intermetallic is reduced, resulted in development of thinner IMC at the interface [9, 15].

Fig. 44 revealed the effect of welding current on thickness of intermetallic layer, in which average reaction layer thickness varies between 1.244 µm and 4.931 µm. In the joint of Al 5052 alloy and Zn coated galvannealed steel, reaction layer thickness decreases with increasing welding current up to 10 kA. Similarly, for joint without cover plate at higher welding currents (> 10 kA). Reason for decrement of reaction layer thickness with increasing current is vaporisation of Zn coat. Evaporation consume more generated heat. Fig. 40 depicts the generation of gas porosity inside the aluminium alloy and at the joint interface due to vaporisation of Zn coat also vaporisation increases with increasing current. Therefore, effective heat devoted for intermetallic growth decreases. Thus, reduction of thickness layer with the increase of welding current as expressed in Fig. 44.

At higher current i.e. at 10.5 kA and 11.0 kA, there is no reaction layer but minimum amount of Al of thickness approx. 6µm is observed. Since at high current Al alloy is completely melted and squeezed out under electrode force. High heat generated in cover plate is directed into steel/Al interface coupled with high heat generated at steel/Al interface is the reason for complete melting and squeeze out of Al alloy.

Table 12

Effect of welding current on thickness of IMCs (central region- with cover plate)

Welding Current (kA)	Thickness of Reaction Layers (Central Region – With Cover Plate) (µm)			Average Thickness of Reaction layer (Central Region- With Cover Plate) (µm)
8.0	4.608	5.248	4.938	4.931
8.5	3.421	3.114	3.367	3.301
9.0	4.082	4.525	3.653	4.087
9.5	3.216	2.688	2.961	2.955
10.0	1.096	1.350	1.286	1.244

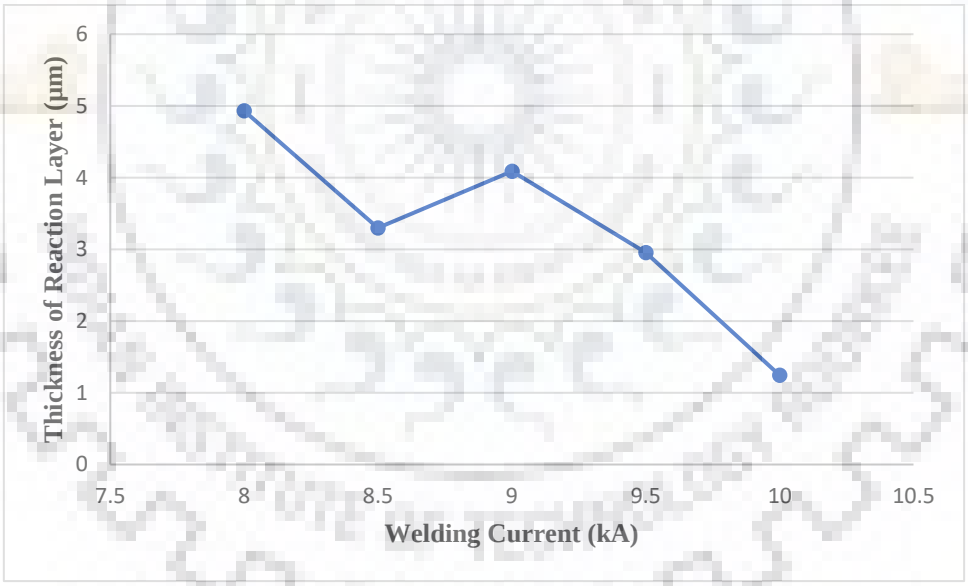

Fig. 44 Effect of welding current on thickness of reaction layer (central region – with cover plate).

4.2.3 Evaluation of joint properties

4.2.3.1 Effect of Welding Current on Nugget Diameter

Fig. 45 (a-i) express the stereoscopic images of fracture surface at different welding current. Nugget diameter is measured from fracture surface of sample failed in shear test as displayed in Fig. 45 (a-i).

Measured value of nugget diameter at different welding current is presented in Table 13, and graph is plotted between average nugget diameter and welding current, as expressed in Fig. 46.

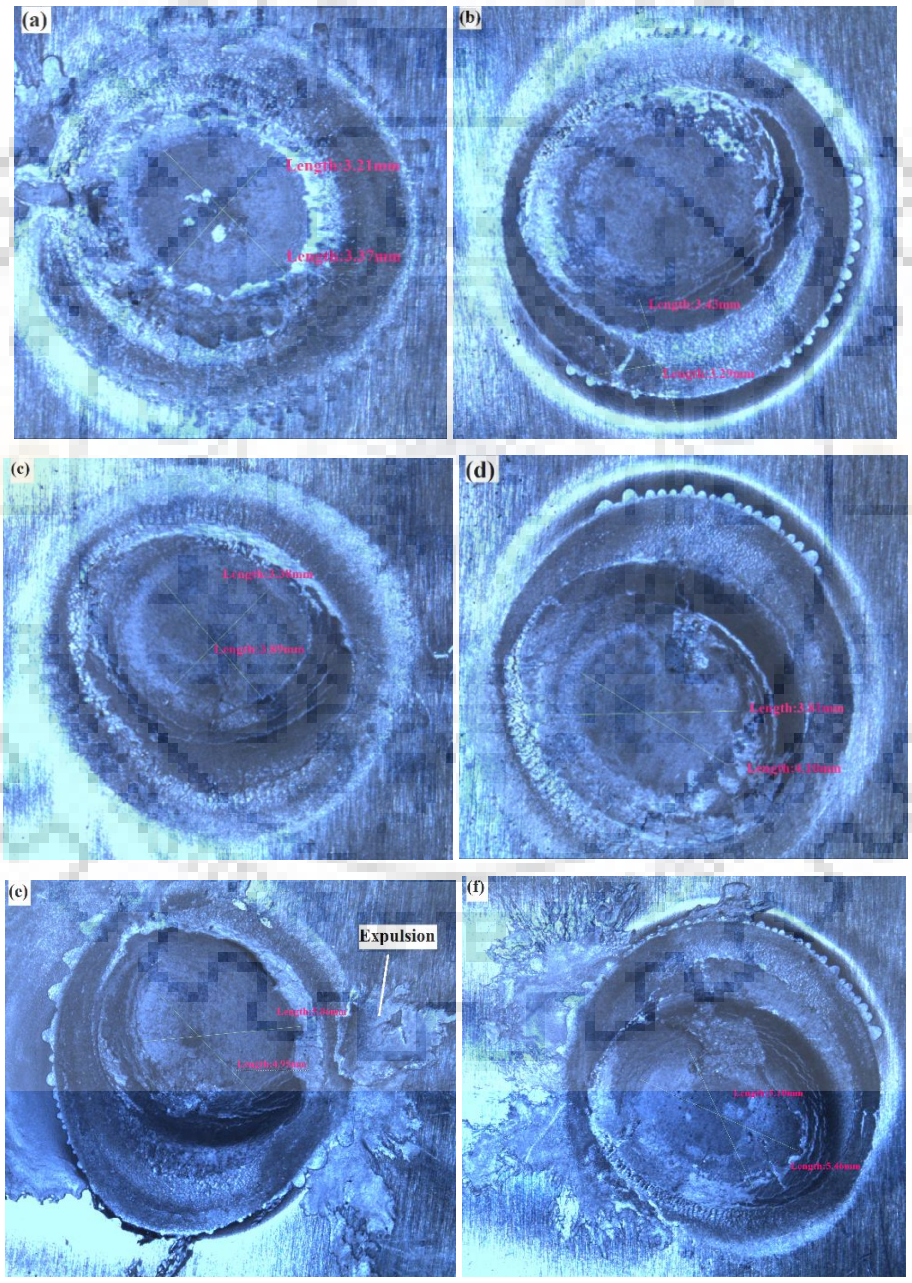

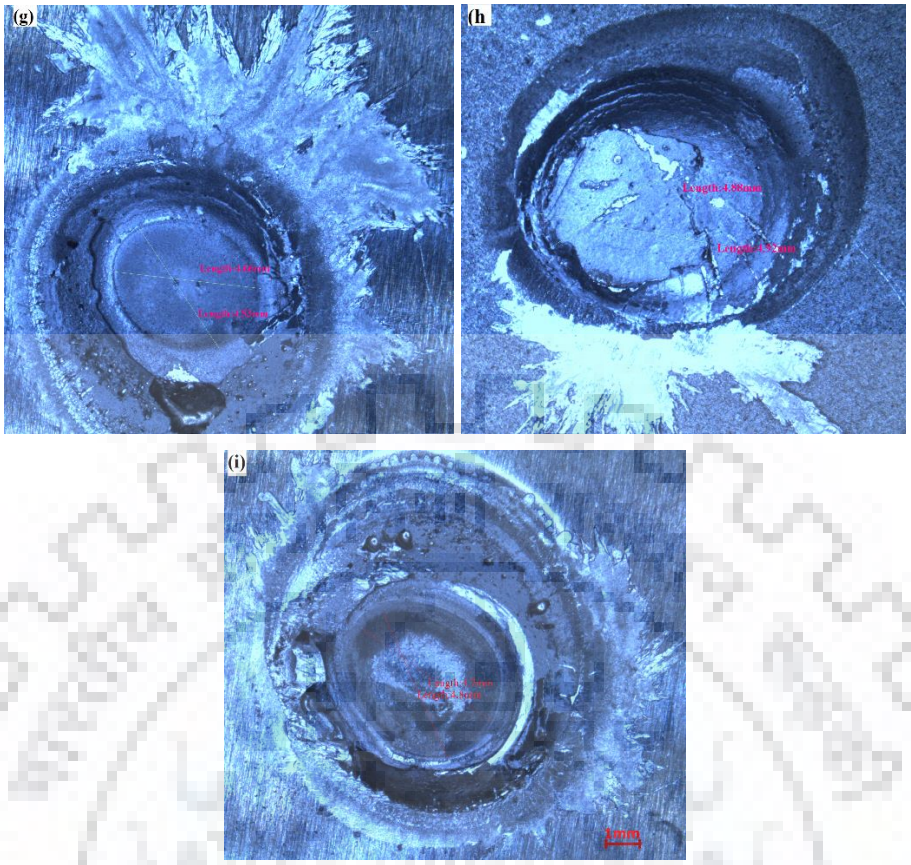

Fig. 45 Fracture surface at (a) 7 kA, (b) 8.0 kA, (c) 8.5 kA, (d) 9.0 kA, (e) 9.5 kA, (f) 10.0 kA, (g) 10.5 kA, (h) 11.0 kA, (i) 11.5 kA - (with cover plate).

Melted nugget volume is a function of heat input at faying surface. Increasing welding cuurent added with heat conduction from cover plate to toward interface increases more heat input, which result in more melted volume. Thus, relatively large increase in nugget diameter comparatively with weld joint of without cover plate. However, growth rate of nugget diameter is not contstant for all current value as expressed in Fig. 46. Nugget diameter increases slowly up to 8.5 kA, followed by dramtic growth of nugget upto 10.0 kA. Maxmimum nugget diameter is 5.28 mm at 10.0 kA. Dramatic growth can be attributed to excess heat input at faying surfaces and least metal expulsion.

Aluminum metal expulsion begins at 9.5 kA as shown in Fig. 45 (e) and expulsion increases with further increase in current as indiacated in Fig. 45. Excessive metal expulsion could be the reason of decrement in nugget diameter for current beyond 10.0 kA.

Table 13

Effect of welding current on nugget diameter - (with cover plate)

Welding Current (kA)	Nugget Diameter (mm)		Average Nugget Diameter (mm)
7.0	3.21	3.37	3.29
8.0	3.50	3.70	3.36
8.5	3.38	3.89	3.64
9.0	3.81	4.10	3.96
9.5	5.06	4.95	5.01
10.0	5.10	5.46	5.28
10.5	4.66	4.53	4.56
11.0	4.88	4.92	4.90
11.5	4.70	4.80	4.75

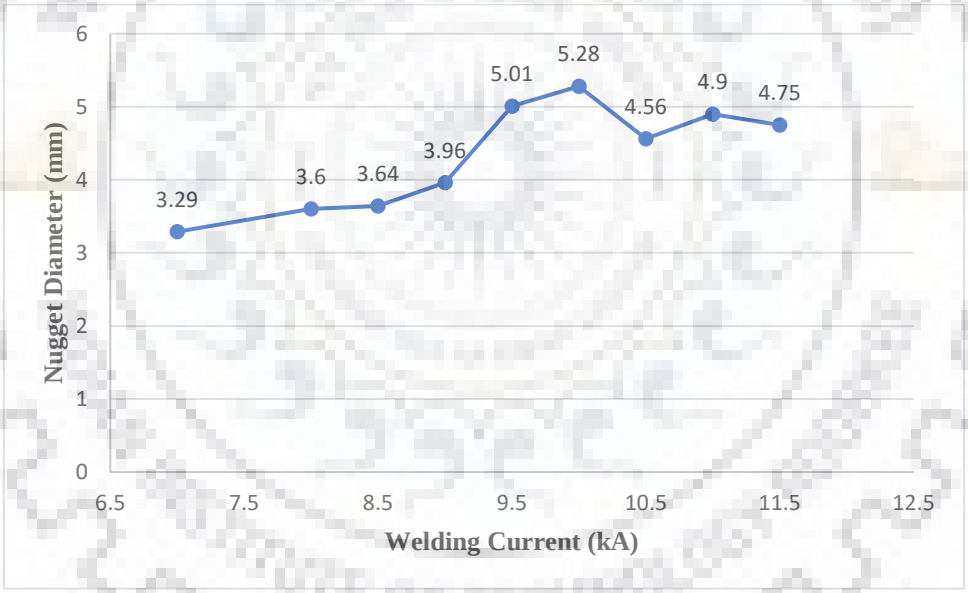

Fig. 46 Effect of welding current on nugget diameter - (with cover plate).

4.2.3.2 Effect of welding current on shear strength of joints

Two samples are being tested on UTM corresponding to each current. Failure load is noted from load- extension curve as represented in Annexure B and values are presented in Table 14. Similarly, variation of average shear strength with increasing current is plotted in Fig. 47.

Results indicates that slope of shear load is not constant for all current. It's increased in a quasi-linear characteristic up to 10.0 kA, at 10.5 kA strength decreased and beyond 10.5 kA shear load have slow growth till 12 kA. Highest joint shear strength is 5675N at 10.0 kA.

Growth of tensile shear load is in good accordance with change in nugget diameter, and intermetallic thickness with increasing current as expressed in Fig. 45 & 47. Reduction of thickness layer and increase of nugget diameter is the reason for drastic improvement in joint shear strength with increasing current up to 10 kA. Decrement in nugget diameter due to excessive metal expulsion and sheet thickness reduction for current beyond 10.0 kA is the reason for reduction of joint strength at 10.0 kA.

Table 14

Effect of welding current on joint shear Load – (with cover plate)

Welding Current (kA)	**Tensile Shear Load (N)**		**Average Tensile Shear Load (N)**
	Sample 1	Sample 2	
7.0	2413	2413	2413
8.0	4652	4600	4626
8.5	4783	4509	4646
9.0	5131	4656	4893.5
9.5	5174	4898	5036
10.0	5881	5469	5675
10.5	4392	4368	4379
11.0	5066	4699	4882.5
11.5	4832	4690	4761
12.0	5258	4650	4954

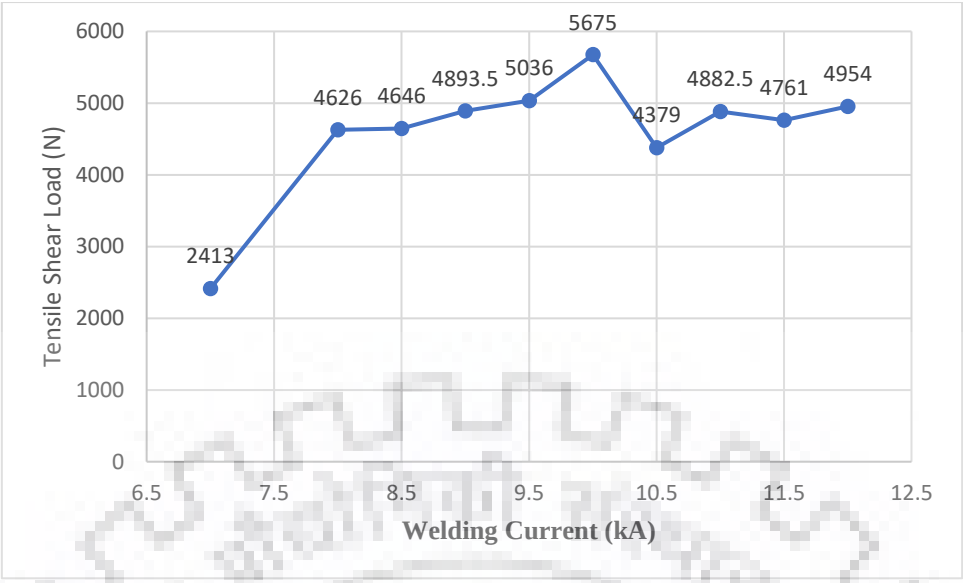

Fig. 47 Effect of welding current on joint shear load – (with cover plate).

4.3 Discussion

Comparisons of joint property of Al5052/galvannealed steel joint - with and without cover plate

4.3.1 Effect of welding current on intermetallic thickness

Fig. 48 expressed that thinner reaction layer are formed for both joint. For joint without cover plate thickness of reaction layer increases slightly with the increasing current up to 10 kA and for higher current (≥ 10.5 kA) thickness of reaction layer decreases with increase of current. Similar trend i.e. reduction of intermetallic thickness with increasing current is reported for joint with cover plate due to Zn coat vaporisation, which consume more latent heat and thus reduces the effective heat for growth of intermetallic layer. Maximum value of intermetallic thickness for joint without cover plate is 5.201µm at 10 kA and for joint with cover plate is 4.931 µm at 8 kA. Zhang et al. [10] reported 7.5- 13 µm intermetallic thickness for high strength GI/Al 6000 series joint.

Table 15

Effect of welding current on reaction layer thickness (with and without cover plate)

Welding Current (kA)	Average Thickness of Reaction layer (Central Region- Without Cover Plate) (µm)	Average Thickness of Reaction layer (Central Region- With Cover Plate) (µm)
8.0	4.330	4.931
8.5	4.630	3.301
9.0	4.684	4.087
9.5	4.440	2.955
10.0	5.201	1.244
10.5	4.371	
11.0	4.099	

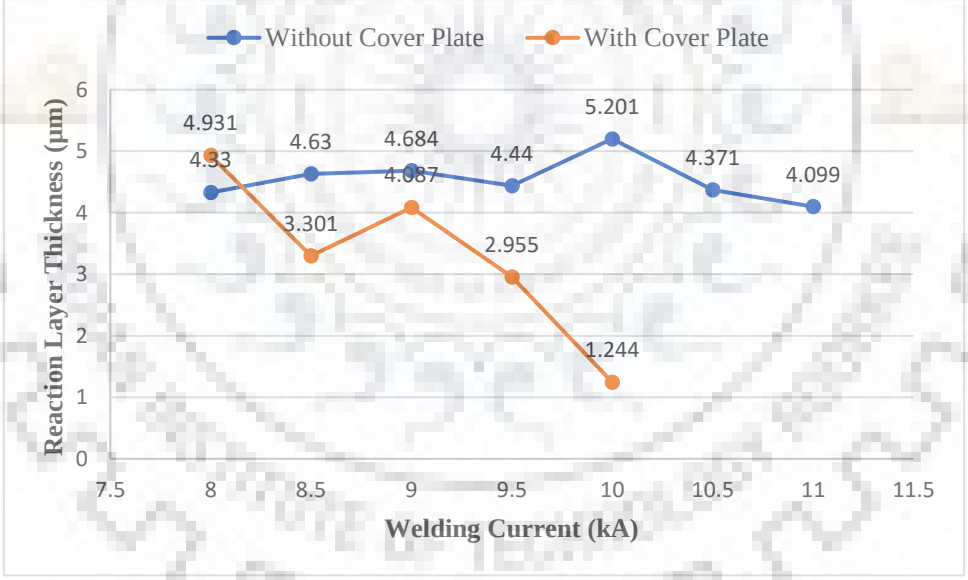

Fig. 48 Effect of welding current on reaction layer thickness.

4.3.2 Effect of welding current on nugget diameter

Fig. 49 expressed that joint with cover plate have higher nugget diameter than join without cover plate due to generation of additional resistance heat at the interface of cover plate/Al joint and directed towards joint of Al/galvannealed steel joint. However, quasi- linear growth of nugget diameter with increase of current up to 9.0 kA is common for both joint. Beyond 9.0 kA, there is dramatic jump in nugget diameter for joint with cover plate for current up to 10.0

kA due to excess heat input at interface and least expulsion and further nugget diameter decreases due to excessive metal expulsion. However, nugget growth rate is very slow for joint without cover plate for current beyond 9.0 kA attributing to reduction in electrical resistance due to growth of nugget size.

Maximum value nugget diameter for joint with cover plate is 5.28 mm at 10.0 kA and 3.81 mm at 11.0 kA for joint without cover plate. i.e. there is 38.58 % improvement in nugget diameter with the use of cover plate. Zhang et al. [10] reported 5.8 mm nugget diameter at 9 kA, 300 ms for high strength GI/Al 6000 series joint.

Table 16

Effect of welding current on nugget diameter (with and without cover plate)

Welding Current (kA)	**Average Nugget Diameter -Without Cover Plate (mm)**	**Average Nugget Diameter -With Cover Plate (mm)**
6.0	2.02	
7.0	2.60	3.29
8.0	3.14	3.36
8.5	3.24	3.64
9.0	3.42	3.96
9.5	3.74	5.01
10.0	3.75	5.28
10.5	3.65	4.56
11.0	3.81	4.90
11.5	3.65	4.75

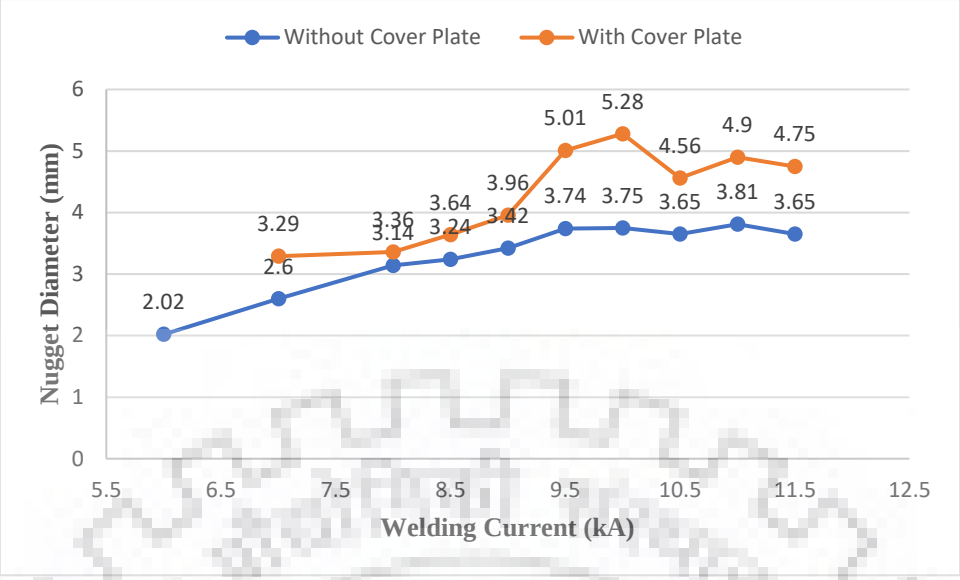

Fig. 49 Effect of welding current on nugget diameter.

4.3.3 Effect of welding current on joint shear load

Fig. 50 revealed that growth of tensile shear load is in accordance with growth of nugget diameter as indicated in Fig. 49. However, decrement in intermetallic thickness and excess improvement of nugget diameter with increasing current due to excess heat at interface by the use of cover plate, is the reason for dramatic improvement of joint strength even at lower temperature for joint with cover plate as expressed in Table 17. Maximum value of tensile shear strength is 5675 N at 10.0 kA for joint with cover plate and 4049.3 N at 11.0 kA for joint without cover plate i.e. 40.14 % improvement in joint shear strength with the use of cover plate. Zhang et al. [10] reported 3309 shear tensile strength at 9 kA, 250 ms for high strength GI/Al 6000 series joint.

Table 17

Effect of welding current on tensile shear load (with and without cover plate)

Welding Current (kA)	Average Tensile Shear Load - Without Cover Plate (N)	Average Tensile Shear Load - With Cover Plate (N)	% Improvement in Joint Shear Strength
7.0	2014.7	2413	19.77
8.0	2963.3	4626	56.11
8.5	3275.0	4646	41.87
9.0	3399.0	4893.5	43.97
9.5	3915.0	5036	28.63
10.0	3853.7	5675	47.26
10.5	3786.3	4379	15.65
11.0	4049.3	4882.5	20.58
11.5	3546.3	4761	34.25
12.0	3358.7	4954	47.50

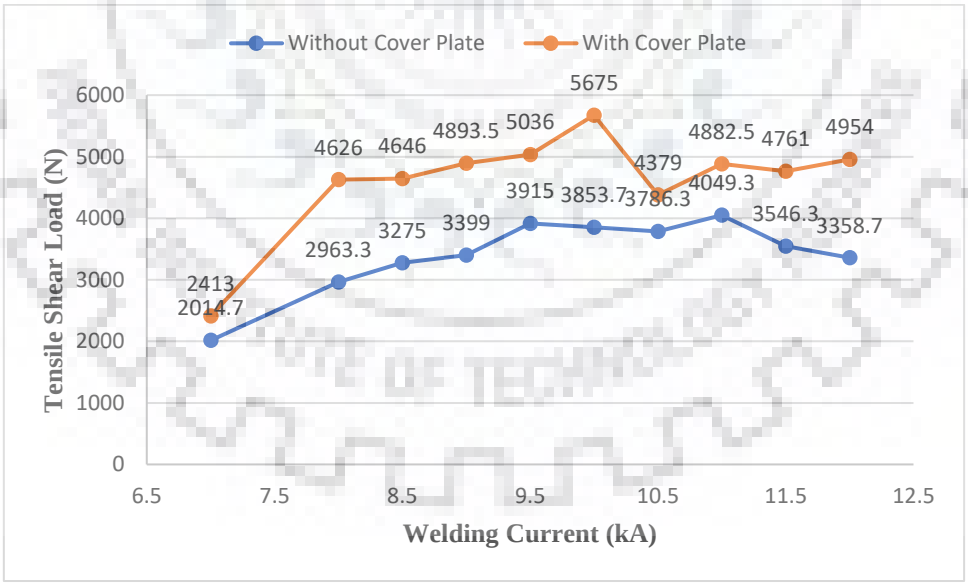

Fig 50. Effect of welding current on tensile shear load.

Conclusions

In the present work, 1.5 mm thick Al 5052- H32 alloy welded with 1.0 mm thick Zn coated galvannealed steel by resistance spot welding with and without use of cover plate (1.0 mm thick CRC steel). Joint properties are assessed by the tensile shear strength of welded joints and microstructure at the interface. Effect of nugget diameter, and thickness of reaction layer on tensile shear strength was discussed. Effect of Zn coating on microstructure and mechanical behaviour of joint was explored.

Cover plate technique is used to concentrate more heat at interface in order to obtain high strength of joint at lower range of current. Outcome of the study is as follows-

i.) Dumbbell shape weld cross section exist for both joints. Thickness of Al alloy decreases with increase of welding current i.e. electrode indentation increases with increasing current at joint location.

ii.) Intermetallic thickness is higher at nugget centre and continuously decreases with the distance from centre for both joints. Reason for this variation in thickness is attributed to the heat distribution in welded region.

iii.) Zn coating ensures thinner and uniform reaction layer due to fluxing action by low temperature eutectic reaction at the interface. Eutectic liquid of Al- Zn containing oxide, formed at nugget periphery by electrode force, and thus leaving a clean steel surface for lower temperature metallurgical bonding.

iv.) Thinner and regular intermetallic thickness is obtained for joint without cover plate. Intermetallic thickness slightly increases with increment of welding current up to 10 kA, and at higher current (> 10kA), its decreases, since at higher current vaporization of Zn occurs which consume more heat, thus resulted in lower effective heat for growth of reaction layer, and morphology becomes irregular towards steel side.

However, thinner reaction layer also obtained for joint with cover plate and its thickness continuously reduces with increase of current.

v.) Nugget diameter increases with increase of welding current up to 10 kA for both joint. However, growth of nugget for joint with cover plate is higher than the joint without cover plate. Maximum value nugget diameter for joint with cover plate is

5.28 mm at 10.0 kA and 3.81 mm at 11.0 kA for joint without cover plate. i.e. there is 38.58 % improvement in nugget diameter with the use of cover plate.

vi.) Increment in tensile shear load is in accordance with growth of nugget diameter for both joint. However, dramatic improvement in shear load for joint with cover plate is reported even at lower temperature range due to decrement in intermetallic thickness and excess improvement in nugget diameter with increase of current. Maximum value of tensile shear strength is 5675 N at 10.0 kA for joint with cover plate and 4049.3 N at 11.0 kA for joint without cover plate i.e. 40.14 % improvement in joint shear strength with the use of cover plate.

References

1. **W. H. Keran**, "Resistance and Solid-State Welding and Other Joining Processes", *Welding Handbook*, Vol. 3, pp. 01- 55, 1980.

2. **S. Xin, E. V. Stephens, M. A. Khaleel, H. Shao, and M. Kimchi,** "Resistance Spot Welding of Aluminum Alloy to Steel with Transition Material-From Process to Performance-Part I: Experimental Study", *Welding Journal – New York*, Vol. 7, pp. 188- 195, 2004.

3. **S. Xin, E. V. Stephens, M. A. Khaleel, H. Shao, and M. Kimchi**, "Resistance Spot Welding of Aluminum Alloy to Steel with Transition Material-From Process to Performance-Part I: Experimental Study", *Welding Journal – New* York, Vol. 7, pp. 197- 202, 2004.

4. **C. L. Tsai, O. A. Jammal, J. C. Papritan, and D. W. Dickinson**, "Modeling of Resistance Spot Weld Nugget Growth", *Welding Journal –USA*, Vol. 2, pp. 47- 54, 1992.

5. **R. Qiu, C. Iwamoto, and S. Satonaka**, "Interfacial Microstructure and Strength of Steel/Aluminum Alloy Joints Welded by Resistance Spot Welding with Cover Plate", *Journal of Materials Processing Technology*, Vol. 8, pp. 4186-4193, 2009.

6. **M. Pouranvari, H. R. Asgari, S. M. Mosavizadch, P. H. Marashi, and Goodarzi**, "Effect of Weld Nugget Size on Overload Failure Mode of Resistance Spot Welds", *Science and Technology of Welding and Joining*, Vol. 12:3, pp. 217-225, 2007.

7. **T. Liyanage, J. Kilbourne, Adrean P. Gerlich, and T. H. North**, "Joint Formation in Dissimilar Al Alloy/Steel and Mg Alloy/Steel Friction Stir Spot Welds", *Science and Technology of Welding and Joining*, Vol. 6, pp. 500-508, 2009.

8. **M. M. Atabaki, M. Nikodinovski, P. Chenier, J. Ma, M. Harooni, and R. Kovacevic**, "Welding of Aluminum Alloys to Steels: An Overview", *Journal for Manufacturing Science and Production*, Vol. 2, pp. 59-78, 2014.

9. **M. Pouranvari,** "Critical Assessment: Dissimilar Resistance Spot Welding of Aluminum/Steel: Challenges and Opportunities", *Materials Science and Technology*, DOI: 10.1080/02670836.2017.1334310, 2017.

10. **W. H. Zhang, X. M. Qiu, D. Q. Sun, and L. J. Han,** "Effect of Resistance Spot Welding Parameters on Microstructure and Mechanical Properties of Dissimilar Material Joints of Galvanised High Strength Steel and Aluminum Alloy", *Science and Technology of Welding and Joining*, Vol.16:2, pp. 153-161, 2011.

11. **K. Ueda, T. Ogura, S. Nishiuchi, K. Miyamoto, T. Nanbu, and A. Hirose,** "Effects of Zn- Based Alloys on Mechanical Properties and Interfacial Microstructures of Steel/Aluminum Alloy Dissimilar Metals Joints Using Resistance Spot Welding", *Materials Transactions*, Vol. 52:5, pp. 967 to 973, 2011.

12. **M. Winnicki, A. Malachowska, M. Korzeniowski, M. Jasiorski, and A. Baszczuk,** "Aluminum to Steel Resistance Spot Welding with Cold Sprayed Interlayer", *Surface Engineering*, DOI: 10.1080/02670844.2016.1271579, 2017.

13. **S. Chantasri , P. Poonnayom , J. Kaewwichit, W. Roybang, and K. Kimapong,** "Effect of Resistance Spot Welding Parameters on AA1100 Aluminum Alloy and SGACD Zinc coated Lap Joint Properties*", International Journal of Advanced Culture Technology*, Vol. 3:1, pp. 153- 160, 2015.

14. **J. Fan, C. Thomy, F. Vollertsen,** "Effect of Thermal Cycle on the Formation of Intermetallic Compounds in Laser Welding of Aluminum-Steel Overlap Joints", *Physics Procedia*, Vol. 12, pp. 134- 141, 2011.

15. **M.R. Arghavani, M. Movahedi, A.H. Kokabi,** "Role of Zinc Layer in Resistance Spot Welding of Aluminium to Steel", *Materals and Design*, Vol. 102, pp. 106- 114, 2016.

16. **A. Gean, S. A. Westgate, J. C. Kucza, J. C. Ehrstom,** "Static and Fatigue Behavior of Spot – Welded 5182- O Aluminum Alloy Sheet", *Welding Journal*, Vol. 78:3, pp. 88- 86, 1999.

Annexure A

Failure load vs displacement curve for three sample at (a) 7.0 kA, (b) 8.0 kA, (c) 8.5 kA, (d) 9.0 kA, (e) 9.5 kA, (f) 10.0 kA, (g) 10.5 kA, (h) 11.0 kA, (i) 11.5 kA, (j) 12.0 kA – (without cover plate).

Sample 1 Sample 2 Sample 3

(a)

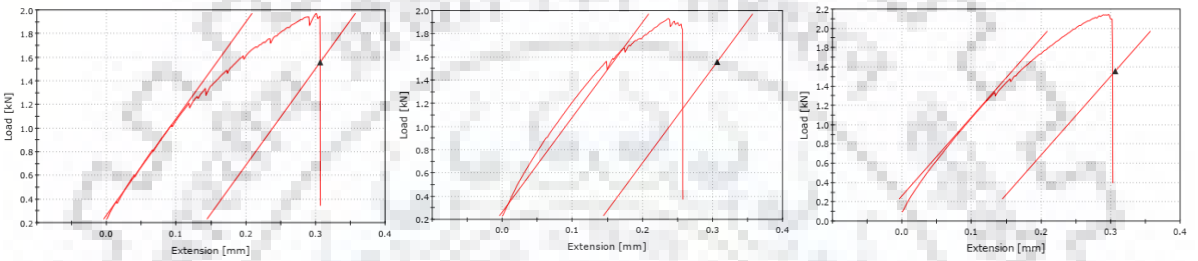

(b)

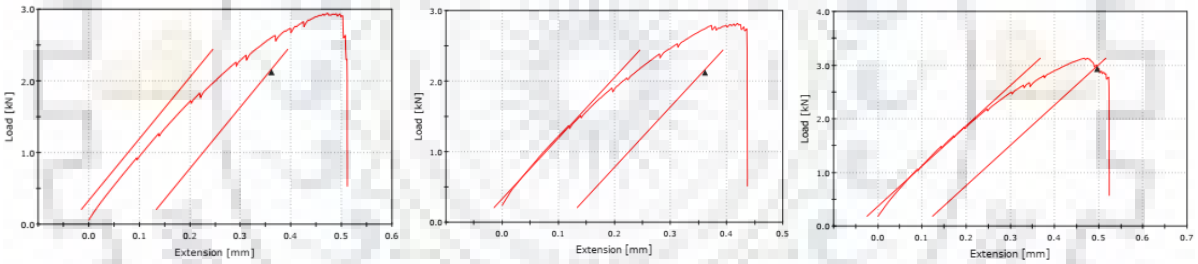

(c)

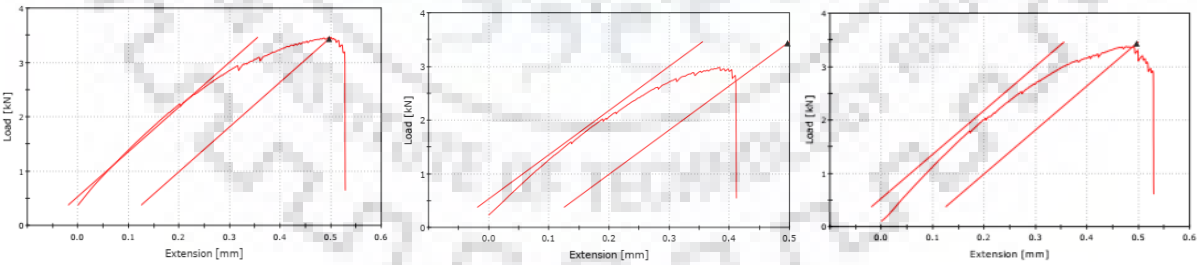

(d)

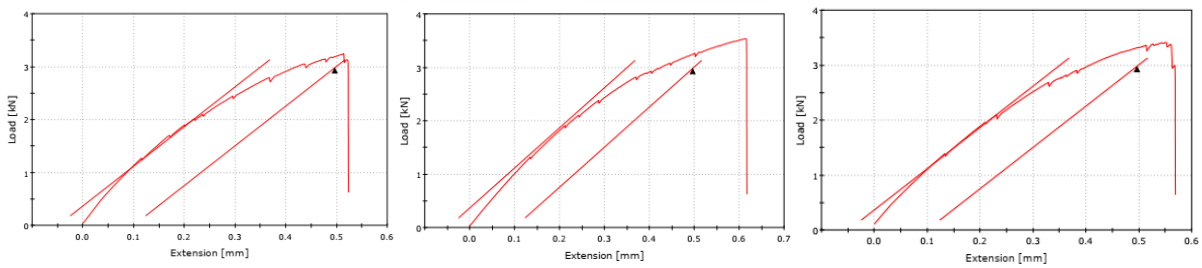

(e)

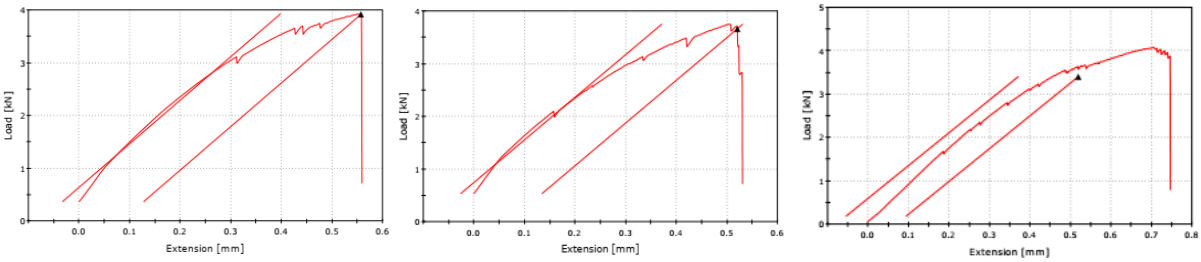
Load [kN]
Extension [mm]

(f)

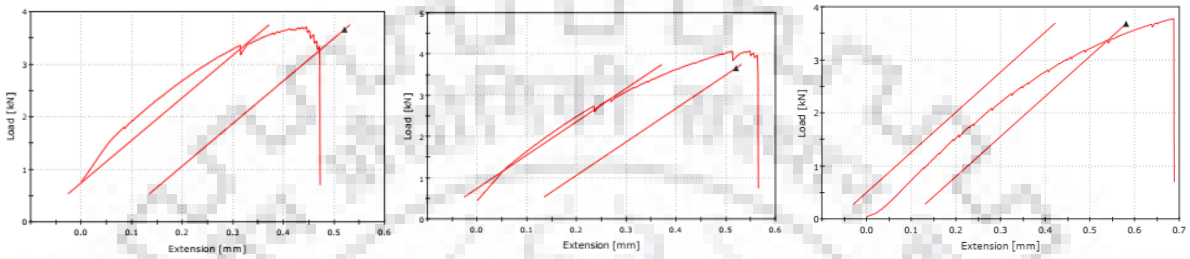
Load [kN]
Extension [mm]

(g)

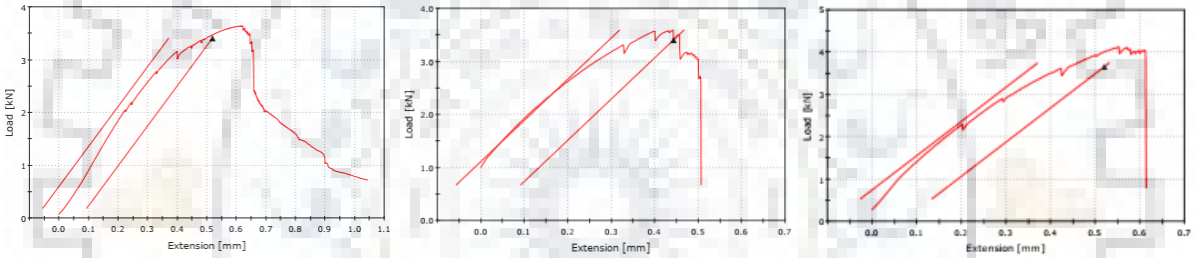
Load [kN]
Extension [mm]

(h)

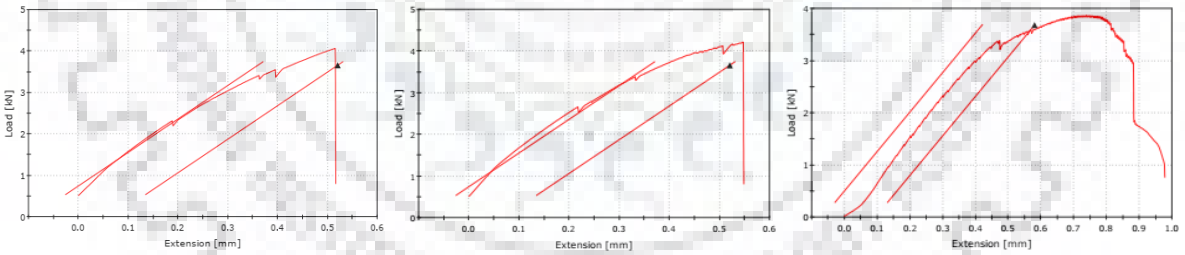
Load [kN]
Extension [mm]

(i)

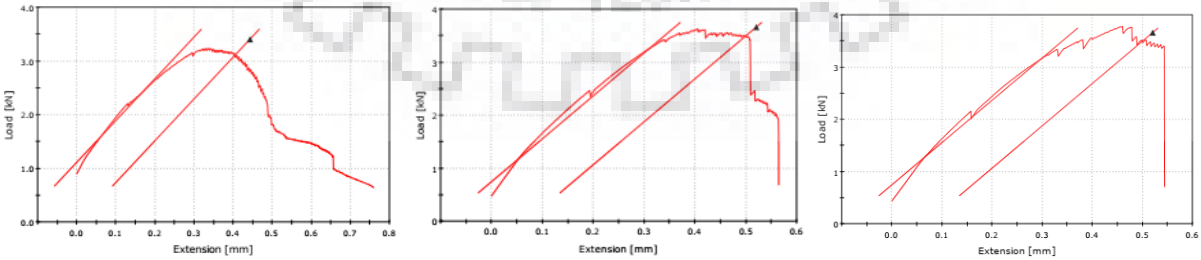
Load [kN]
Extension [mm]

(j)

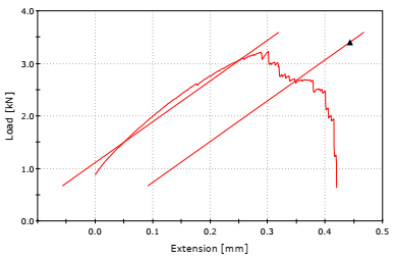
Load [kN]
Extension [mm]

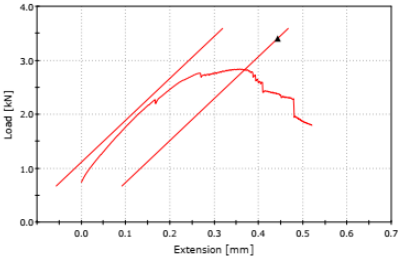
Load [kN]
Extension [mm]

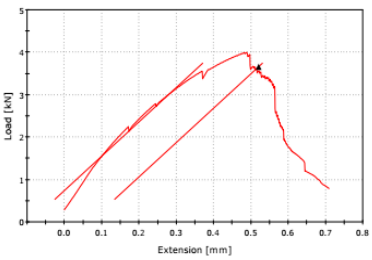
Load [kN]
Extension [mm]

Annexure B

Failure load vs displacement curve for two sample at (a) 8.0 kA, (b) 8.5 kA, (c) 9.0 kA, (d) 9.5 kA, (e) 10.0 kA, (f) 10.5 kA, (g) 11.0 kA, (h) 11.5 kA, (i) 12.0 kA – (with cover plate).

Sample 1 Sample 2

(a)

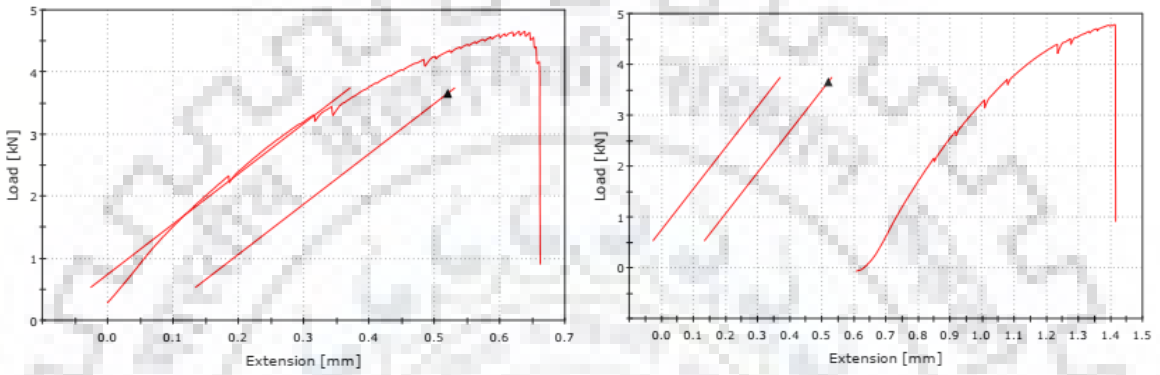

(b)

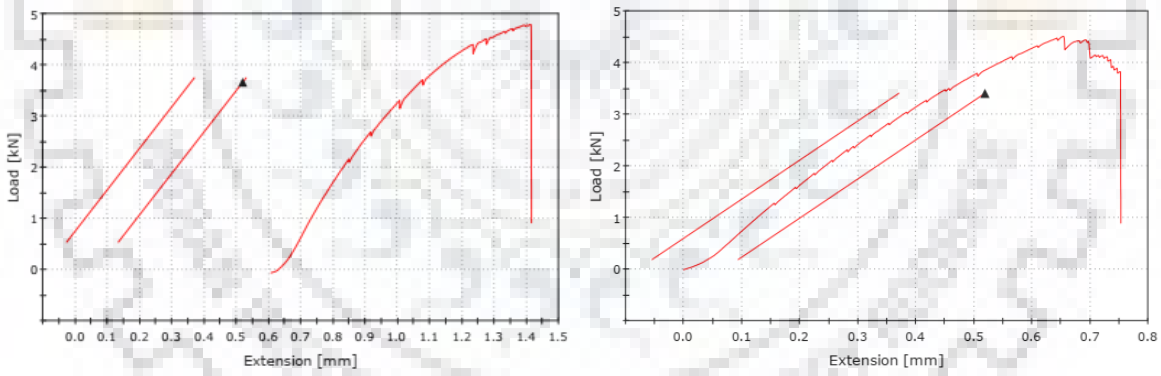

(c)

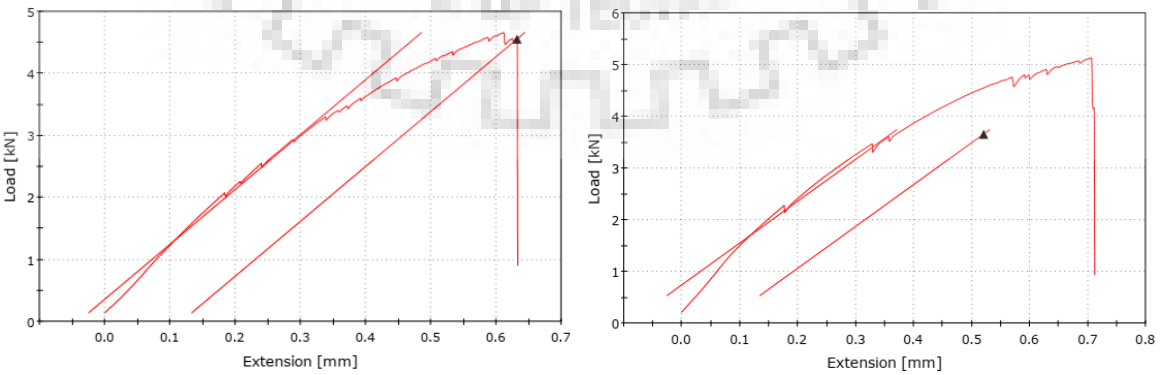

(d)

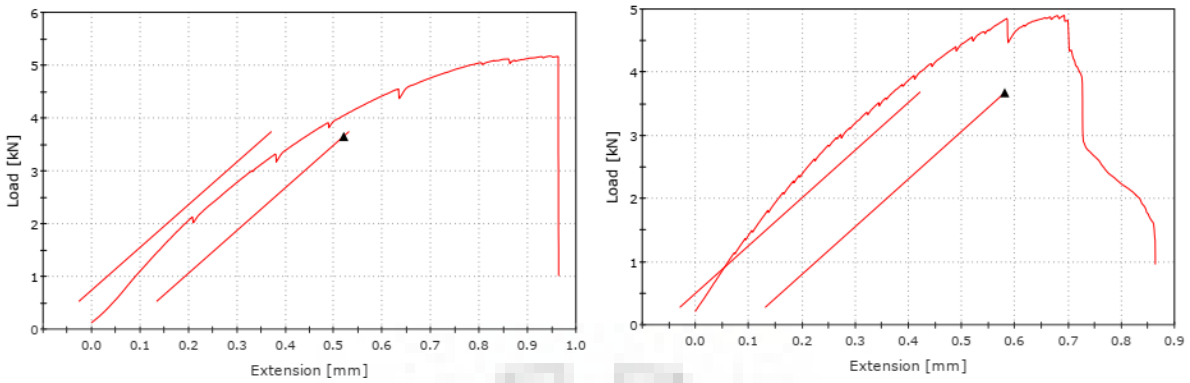
Load [kN]
Extension [mm]
Load [kN]
Extension [mm]

(e)

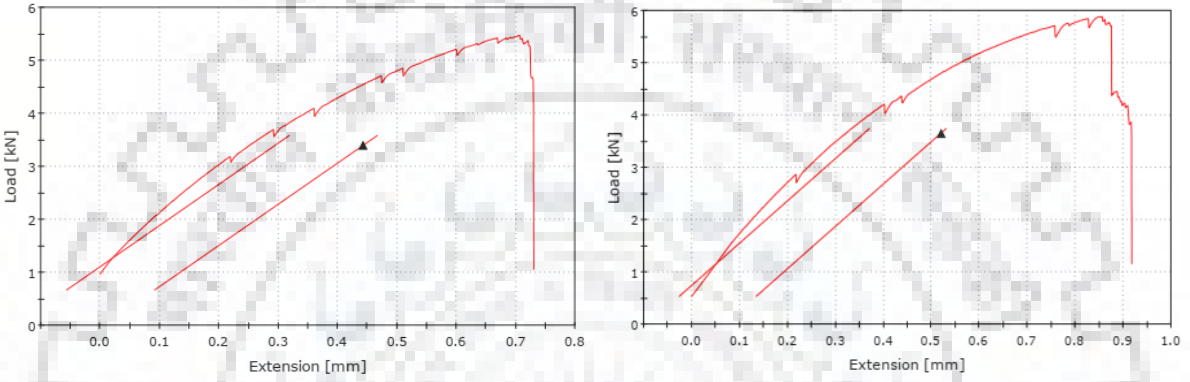
Load [kN]
Extension [mm]
Load [kN]
Extension [mm]

(f)

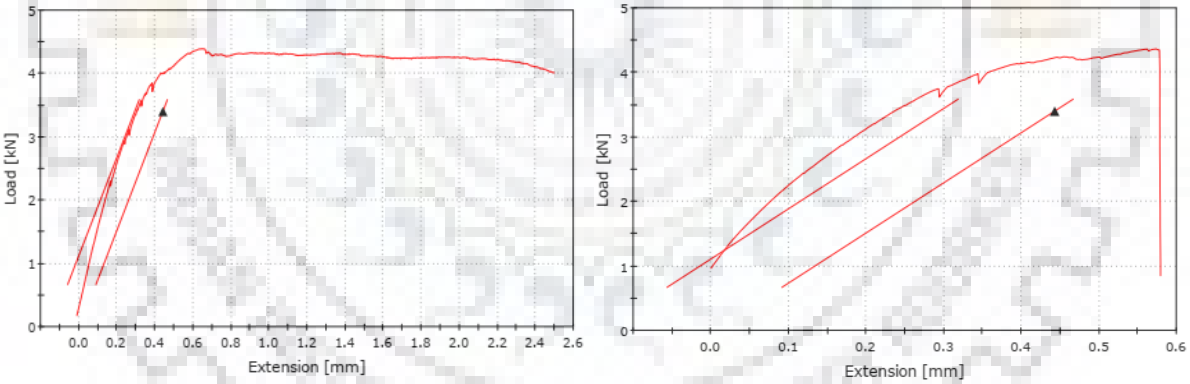
Load [kN]
Extension [mm]
Load [kN]
Extension [mm]

(g)

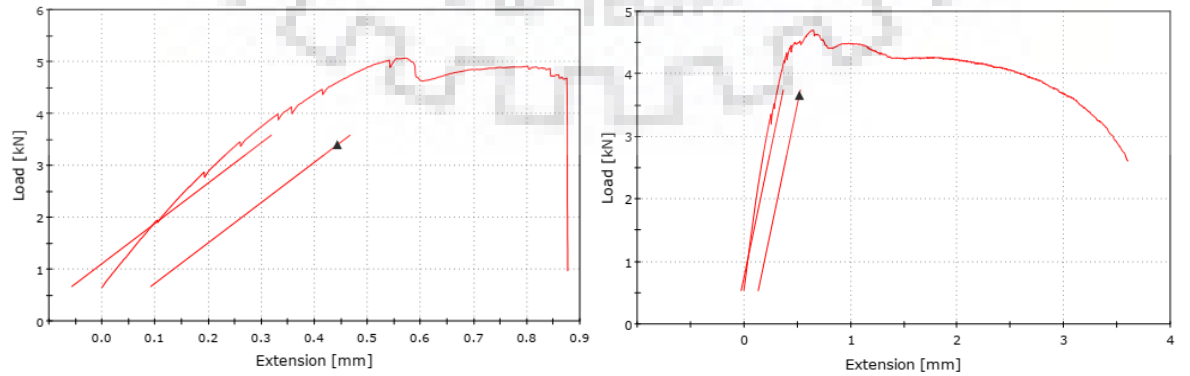
Load [kN]
Extension [mm]
Load [kN]
Extension [mm]

(h)

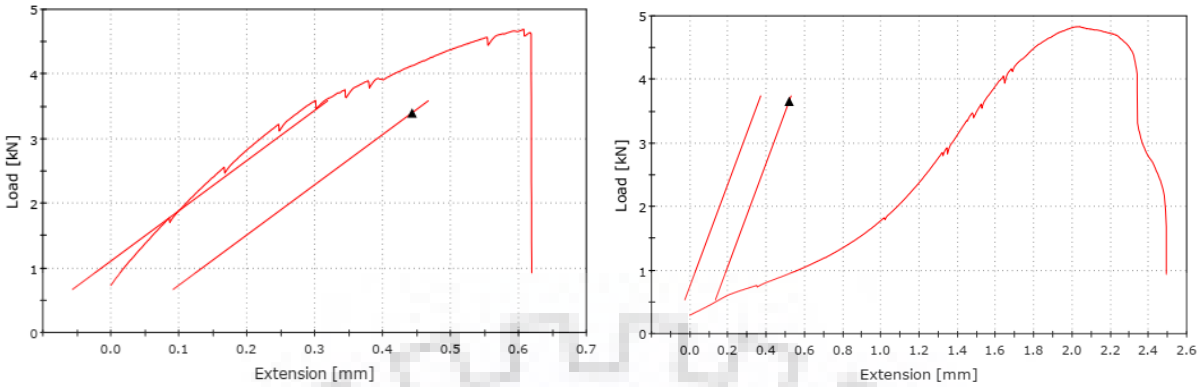
Load [kN]
Extension [mm]
Load [kN]
Extension [mm]

(i)

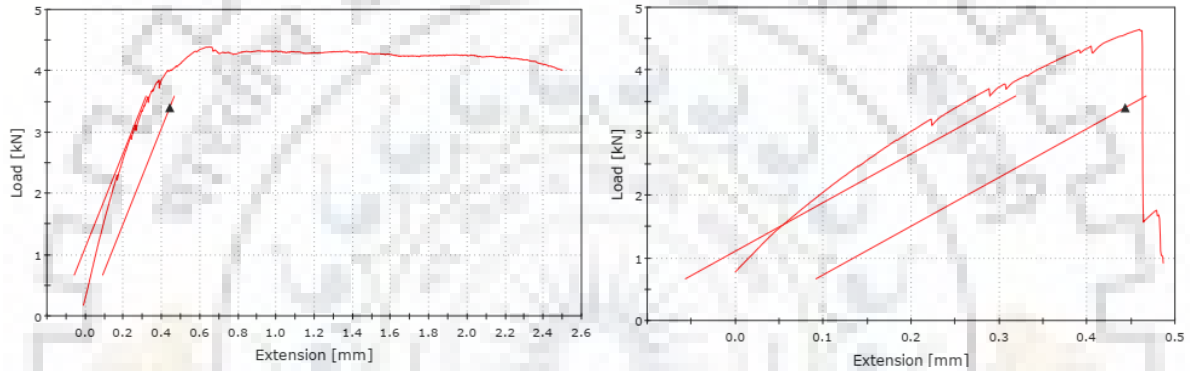
Load [kN]
Extension [mm]
Load [kN]
Extension [mm]